國立台灣師範大學生命科學系 碩士論文

評估 SAHA 及 L-BMX 對 SCA17 小鼠之治療潛力

Evaluation of the therapeutic potential of SAHA and L-BMX on SCA17 mice

研究生：許振銘

Chen-Ming Hsu

指導教授：謝秀梅　博士

Hsiu-Mei Hsieh, Ph.D.

中華民國一０一年二月

Index

摘要

脊隨小腦萎縮症第十七型(SCA17)是一種晚發型的神經退化性疾病，造成疾病的原因是因為人類第六對染色體上面 TATA-box binding protein (TBP) 這個基因有不正常 CAG/CAA 三核甘酸擴增的現象，進而導致轉譯出對於細胞有毒的 polyQ 蛋白，而使得中樞神經性統的細胞死亡。SCA17 臨床上的病症類似於漢丁頓是舞蹈症(HD)，病人會有運動失調、肌張力不足、認知障礙、精神疾病、失智症及舞蹈症等等。

目前有一些治療的方針是針對基因的調控做標的，像是核染色質的乙烯化，就廣泛的被應用在癌症的研究上。在先前的研究中，不管是在動物體或是細胞研究中，組蛋白去乙烯酶的抑制物(HDACi)被發現具有神經保護的功效，因此我們想研究這個治療方式是否也是有利於 SCA17 的治療，我們選用了兩支抑制物，SHAH 是臨床上已經在使用的藥物，以及另一支新穎的 HDAC 抑制物 L-BMX。

在我們的結果中顯示，長期投予這兩支 HDAC 抑制物，對於 SCA17 皆有輕微的治療成效，在病理組織切片的分析中，我們發現投予藥物後，小鼠腦部發炎的情況有顯著的改善，而小鼠運動行為分析上，在比較和緩的分析實驗中，我們可以看到小鼠的步伐以及平衡木上的平衡測試，也都有輕微改善的結果。因此，這兩支藥物確實對於 SCA17 小鼠的治療有輕微的成效。

此外，我們也另外做了 SACA17 小鼠早期的病理分析以及小腦中各種細胞的超微結構觀察，發現 Purkinje cell 細胞除了細胞核有不規則萎縮的情況外，在軸突的部分也有明顯的結構鬆脫，可能會進而導致訊號傳遞的失常及細胞死亡;另外我們也發現早期小鼠腦部發炎的狀況，也可能引起神經細胞的壓力而導致其死亡。

關鍵字：脊隨小腦萎縮症、組蛋白去乙烯酶

Abbreviation list

Abbreviation	Full name
AD	Alzheimer’s disease
ALS	amyotrophiclateral sclerosis
CNS	central nerve system
DAPI	4',6-diamidino-2-phenylindole
DMSO	Dimethyl sulfoxide
EM	electron microscope
HAT	histone acetyltransferase
HSP	heat shock protein
NPC	neural precursor cell
SAHA	suberoylanilide hydroxamic acid
SB	sodium butyrate
SMA	Spinal muscular atrophy
TSA	trichostatin A
VPA	valproic acid
WT	wild type

Abstract

Spinocerebellar ataxias (SCA) 17, is a late onset neurodegenerative disease caused by abnormal CAG/CAA overexpansion in the coding region of the TATA-box binding protein (TBP) gene on chromosome 6q27. The N-terminal polyglutamine (polyQ) overexpansion of TBP leads to intercellular toxicity in central nervous system. The symptoms of SCA17 patients are similar to that of Huntington's disease (HD), including ataxia, seizure, cognitive dysfunctions, psychiatric symptoms, dystonia, and chorea.

The epigenetic regulation of chromatin modification, such as histone acetylation, is widely used in cancer therapy. In recently study, histone deacetylase inhibitors (HDACi) was shown to play a role in neuron protection both in vivo and in vitro. In this study, we applied a widely-used HDACi, suberoylanilide hydroxamic acid (SAHA), and a novel HDACi, L-BMX, on the hTBP-109Q transgenic (TG) mice to assess their therapeutic potential on SCA17.

Our preliminary result showed these two HDACi treatment have mild therapeutic effect on cerebella pathology of transgenic mice through immunostaining analyses. Behavior test with rotarod showed that animals could not benefit from the long-term treatment of these two HDACi compounds. However, under the low strength behavior tests, footprint and beam test, mice showed better performance with SAHA or L-BMX treatment than the non-treated TG control mice. These results revealed that SAHA and L-BMX might have mild beneficial effect on SCA17 mice.

In addition, to further elucidate the neuropathology of the hTBP-109Q transgenic mice, we used immunofluorescent staining and electron microscope (EM) analyses to study the pathological profile of mouse cerebellum and Purkinje cells, respectively. These data should provide us more information for the pathogenesis and therapeutic design for SCA17.

Keyword：SCA17、HDAC inhibitor、SAHA

Introduction

Autosomal dominant cerebellar ataxias (ADCAs)

According to the clinical symptoms, Dr. Harding classified ADCAs into three types, including ADCA type I, II, and III (Harding, 1982). ADCA type I is characterized with pure cerebellar syndrome, including SCA5, SCA6, SCA11, SCA26, SCA29, SCA30, and SCA31. ADCA type II is associated with pigmentary maculopathies and only SCA7 is involved. ADCA type I consist of SCA1- SCA4, SCA8, SCA10, SCA12-SCA23, SCA25, SCA27, SCA28 and dentatorubral-pallidoluysian atrophy (DRPLA), the symptoms are not only located in cerebella and brainstem but also in cerebrum, leads to the feature of dementia, dyschronometria, dyssynergia, dysdiadochokinesia, action tremors, cognitive impairment, cerebellar or supranuclear ophthalmologic signs, peripheral nerve disease, seizure disorders, and psychiatric problems (Whaley et al., 2011).

Spinal cerebellar ataxias type 17

SCA17, also called Huntington's disease like 4, is a neurodegenerative disorder characterized by progressive degeneration of cerebrum, cerebellum, and brainstem. The clinical symptoms includeataxia, dementia, psychiatric disorders, spasticity, epilepsy, bradykinesia, dystonia, and cognitive impairment (Dohlinger et al., 2008). SCA17 is caused by an abnormal CAG/CAA repeat expansion in the TATA-box binding protein-gene (*TBP*) on chromosome 6q27 (Koide et al., 1999). In human, the normal repeat range of CAG/CAA is reported

from 25 to 42 (Stevanin and Brice, 2008). When the repeat number is over 43, it might be associated to familial or sporadic SCA17 (Nakamura et al., 2001; Zuhlke et al., 2001; Reid et al., 2003). There is a linear correlation between the repeat number of CAG/CAA and the age of onset (Nakamura et al., 2001; van Roon-Mom et al., 2005).

The abnormal CAG trinucleotide expansion encodes a long polyQ stretch of disease proteins and cause neurodegenerative disease, including SCA1, SCA3, SCA6, SCA7, SCA8, SCA17, DRPLA, and HD (Trottier et al., 1995; Zoghbi and Orr, 2000; Manto, 2005; Daughters et al., 2009), socalled polyQ diseases. The polyQ expansion leads proteins to a misfolding structure and in turn forms intracellular aggregation and/or nuclear inclusion, which shows a gain of toxic function mechanism including mitochondrial dysfunction, oxidative stress, and transcription alteration (Schaffar et al., 2004; Lin and Beal, 2006; Friedman et al., 2007; Shah et al., 2009). In SCA17,TBP is indispensable required by nuclear RNA polymerases for the initiation of transcription.There have been reported that mutant TBP affects gene expression by enhanced interaction between TBP and transcripition factors, TFIIB and NF-YA, caused the expression level of small shock protein (HSPB1), HSP27, and TrkA downregulation (Friedman et al., 2008; Shah et al., 2009; Huang et al., 2011). Chaperons are known to help protein refold and against oxidavite stress, which its dounregulation will be resulted in neuron toxicity.

Inflammation and microglia

In human brain, neuroinflammation always associated with microglia activation by bacterial, viral infection, head trauma, autoimmune disease or neurodegenerative disease. The phenotype of microglia activation was demonstrated in the early 20th century by RíoHortega in the healthy and diseased brain. There are many studies about microglia, including acute and chronic neurodegenerative disorder conditions (Jack et al., 2005; Moisse and Strong, 2006; Pavese et al., 2006; Kaindl et al., 2009; Morgan, 2009; Yadav and Collman, 2009; Weinstein et al., 2010).

Microglia, act as macrophages, are the resident immune cell in central nerve system (CNS). The greatest number was found in the hippocampus, basal ganglia, substantianigra, and lower density in cerebellum and brainstem (Savchenko et al., 2000). It plays an important role in the neuroprotective mechanism but also can aggravate neurodegenerative process. The neuroprotective mechanism of microglia may be mediated by releasing of neurotrophins, NGF and BDNF, and interleukins, IL-3 and IL-6 (Inoue and Tsuda, 2009; Napoli and Neumann, 2009). Neurotoxic effect may be mediated by releasing of glutamate, TNFα, or NO (Lambertsen et al., 2009).

In the study of acute activation of microglia, it showed reduced neural precursor cell (NPC) population, decreased neuronal differentiation and promoted NPC underwent glial fate. On the other hand, chronically activated microglia could help for NPCs survival, and neuronal differentiation (Ajmone-Cat et al., 2010).

Histone deacetylase inhibitor (HDACi)

Transcription is regulated by multiple modulation of histone such as acetylation, methylation, and phosphorylation. Histone acetylation is determined by interplay between histone deacetylases (HDACs) and histone acetyltransferases (HATs) to modify chromatin and regulate transcription (Marks et al., 2001). Histone acetylation results in relaxed chromatin conformation that is tended to transcription activation. In contrast, histone deacetylation associates with tightly conformational chromatin and represses gene expression.

There are 18 HDACs in mammalian and which are divided into four classes, class I, II, III, and IV, which were based on sequence homology to their yeast HDACs (Marks and Dokmanovic, 2005; Yang and Seto, 2008).The class I, II, and IV HDACs are zinc-dependent hydrolases, but class III HDACs are nicotinamide adenine dinucleotide (NAD^+)-dependent enzymes. The class I HDACs including HDAC1, 2, 3, and 8. There has been reported that HDAC2 plays a role of negative regulation in memory formation (Guan et al., 2009).The classes II HDACs were divided into two subclasses, IIa including HDAC4, 5, 7,9,and IIb including HDAC6 and 10, according to their similarities of structure. There has been reported that HDAC5 plays a role of antidepressant action (Tsankova et al., 2006) and chronic emotional stimuli (Renthal et al., 2007). The class V HDAC, HDAC11, was identified by its distinct structure (Voelter-Mahlknecht et al., 2005). In contrast, the class IV HDACs, sirtuins (SIRT), including SIRT1-7 (Michishita et al., 2005), which were associated with aging and could

extend life span in TG mouse model (Alcendor et al., 2007; Donmez and Guarente, 2010). However, about the role of HDACs involved in signaling transduction pathways and posttranslational modifications are largely unknown.

HDAC inhibitors, the common studied compounds such as SAHA, valproic acid (VPA), trichostatin A (TSA), sodium butyrate (SB), and phenylbutyrate, were used in several neurodegenerative disease like Alzheimer's disease (AD), HD, amyotrophiclateral sclerosis (ALS), Spinal muscular atrophy (SMA), and cerebral ischemia (Steffan et al., 2001; Ferrante et al., 2003; Hockly et al., 2003; Ryu et al., 2005; Fischer et al., 2007; Tsai et al., 2008; Guan et al., 2009; Kim et al., 2009). In HD models, from *Drosophila* to vertebrate, HDAC inhibitors could slow down pathogenesis (Steffan et al., 2001). In HD *Drosophila* model, larvae treatment with SAHA or TSA could decrease the photoreceptor degeneration in the eyes and reduced the adult death (Steffan et al., 2001). In HD TG mouse models, animals treated with SAHA or SB could improve behavior performance, survival rate, and decrease the neurodegeneration phenotype (Steffan et al., 2001).

HDACs also associated with synaptic plasticity, learning and spatial memory formation (Fischer et al., 2007). The AD-like mice with CK-p25 inducible expression were treated with SB, and their dementia phenotype in water maze and the number of synapse were improved by the treatment (Fischer et al., 2007). In ALS TG mouse model, animals administered phenylbutyrate or VPA extended survival rate and improved pathological phenotypes (Ryu et al., 2005). In SMA study, TG animals administered

VPA improved motor function and suppressed spinal motor neuron loss (Tsai et al., 2008). Furthermore, a recent study reported that rats long-term administered SB could promote neurogenesis by BDNF signaling pathway (Kim et al., 2009). Therefore, HDAC inhibitors might be a potential therapy in SCA17 in helping to restore transcription.

Materials and Methods

SCA17 transgenic mice

We have established a transgenic mice, human TBP with 109-glutamine (109Q) expanded driven by pcp2/L7 promoter in FVB background. Mice were breed in the chamber with abundance food and water in a 12-h light (0700-1900) and 12-h dark (1900-0700) cycle in IVC system (LASCO, Taiwan).

Tail DNA extraction

The 0.2-0.3 cm mouse tail biopsies were mined in 200 μl tail solution (100 mM Tris PH 8.0, 200mM NaCl, 5mM EDTA PH 8.0, 0.2% SDS, 1.5M proteinase K) then incubated at 65℃ overnight. The mixture were mixed 80 μl 5M potassium acetate (KOAc) and placed on ice for 1 hour, centrifuged at 12,000×g for 30 min. The supernatant were collected to a new eppendorf and mixed with 1 ml pure ethanol.

Drug administration

Animals were administrated intraperitoneal injection daily (50 μl) with a 17 mg/kg of SAHA or 25 mg/kg of L-BMX, dissolved in Dimethyl sulfoxide (DMSO) (Sigma, St. Louis, USA) and cremophor EL (Sigma, St. Louis, USA) and made fresh daily from the age of 4 weeks to 20 weeks. Control littermates were treated with DMSO and cremopher EL only.

Animal behavior test

A. Rotarod

The rotarod (UGO 47600, Ugo Basile, Italy) apparatus consists of a 28 mm diameter rod partitioned into five lanes 58 mm wide to accommodate individual mice. The rod was positioned 30 cm above a surface. Before test, mice were handled approximate 5 minutes to reduce their anxiety four consecutive days. At the first experiment, mice were pre-trained in the first two days as the acceleration speed of 4~30 rpm for 300 seconds then fixed 40 rpm for next 300 seconds. After training, mice were used the same condition for testing in the next two days. Each experiment was included three trials per day and the mice should be taken a break at least 40 minutes between trials.

B. Locomotion activity

Mice were placed in a 30 cm × 30 cm × 30 cm open field of black box. Each experiment was included two trials per 300 seconds. Etho-Vision video tracking system (Noldus, Nederland) was used to assess their movement ability.

C. Beam test

Mice were trained to walk on a wood (3 cm wild, 50 cm long) elevated 35 cm above the litter by acrylic supports with a platform in the terminus. Three trials were tested for each mouse to make sure they were aware that there was a safety platform could be reached. This 3 cm wild beam was used because mice could cross it easily and would not induce their anxiety. After the pre-training, mice were moved immediately to the beam test. The beam (0.8 cm wild, 65 cm long)

elevated 40 cm above the litter by acrylic supports. Mice were placed on the start end and allowed to walk to the platform during 60 seconds. If mice fell, they would be placed on the position that they fell from. The measurement taken included the time on the beam and the number of foot slips.

D. Footprint

The forelimbs of mouse were painted red and its hindlimbs were painted blue then allow mice walked on the 5 cm × 60 cm lane. The lane was laid rice paper to record its footprint.

Western blot analysis

Cerebellum tissue were homogenized in 10 volumes of RIPA (1M Tris pH 7.5, 5M NaCl, 0.5M EDTA pH 8.0, 10% SDS, 10% DOS, and 10% NP40) including protease inhibitor. Samples were placed on ice for 5 min, centrifuged at 12,000×g for 20 min at 4 ℃ and collected the supernatant. The lysate were quantified by ABC kit. Equal amounts of the protein samples were applied on 8~12 % SDS-PAGE gels and proteins were transferred to nitrocellulose membranes (Hybond-ECL, Amersham Biosciences, USA). Western blots were hybridization with primary antibody overnight at 4℃, then incubated in secondary antibodies, donkey anti-mouse (Invitrogen, Carlsbad, USA), donkey anti-rabbit (Invitrogen, Carlsbad, USA).

Immunohistochemistry stain

Mice were anaesthetized and transcardially perfusion with 0.9% normal saline followed by 4% paraformaldehyde (PFA). Brain tissues were fixed in 4% paraformaldehyde for 4 hours, and then soaked in 30% sucrose for 24–48 hours for frozen sectioning (20 μm). After blocking (4% BSA), the brain sections were incubated with primary antibody diluted with blocking solution overnight at room temperature. Then sections were washed with PBST (contain 0.2% triton X-100) and the secondary antibody were applied to the sections by linking reagent (DAKO, Denmark) for 1 hour. Immunostainings were highlighted by substrate-chromogen solution and diaminobenzidine (DAB) oxidation (DAKO) for 3 second to 3 minutes.

Immunofluorescence stain

Brain tissue preparation were performed as Immunohistochemistry stain described. After blocking (4% BSA), the brain sections were incubated with primary antibody diluted with blocking solution overnight at 4℃. Then sections were washed with PBST (contain 0.2% triton X-100) and incubated with the secondary antibody for 1 hour at room temperature. Then sections were washed by PBST contain 4',6-diamidino-2-phenylindole (DAPI) for 15 minutes and another three times wash with PBST for 10 minutes.

Result

Part 1. Characterization of SCA17 cerebellar pathology.

hTBP-109Q transgenic mice showed a progressive Purkinje cell loss in the cerebellum

Calbindin staining highlights Purkinje cells in the cerebellum. No significant reduction was observed in the Purkinje cells between wild type (WT) and TG mice at 4 weeks. At 6 weeks old, Purkinje cell loss could be found in the TG mice, and it's more serious at 8 weeks old TG mice (Figure 1).

The gliosis pattern in TG mouse cerebella

GFAP staining highlights the astrocytes. We observed that astrocyte activation was found in TG mouse cerebella at 6 weeks old (Figure 2). S100 staining was conducted to highlight the Bergmann glia around the Purkinje cells. Our results showed that S100 signal in TG cerebella was similar to WT at 4 weeks old; however, at 6 and 8 weeks old, the S100 signal was increase (Figure 3A) and the Purkinje cell layer showed higher density of the green signal representing the Bergmann glia process (Figure 3B). In addition, TEM analyses showed that white glia process, the Bergmann glia process, was increased surrounded the Purkinje cells (Figure 3C). These data consistently showed that the process of Bergmann glia was increased in TG mice.

Neuroinflammation in TG mouse cerebella

Iba1 staining highlights the microglia. We observed that TG mouse cerebella suffered from microglia activation started at 4 weeks old (Figure 4A). In addition, this phenomenon was more severe in two sides of cerebellum (lobes 1~3 and 8~10) than center region (lobes 4~7) of cerebellum at 4 weeks old (Figure 4B).

Ultrastructure of TG mouse Purkinje cells

To further characterize the more detail organelle structure phenotypes in the Purkinje cells of the TG mouse cerebellum, we conducted EM analyses on the cerebella of WT and TG mice. First of all, we observed that nuclei showed twisted morphology in Purkinjecell in TG mouse cerebellum compared to the rounded smooth morphology of WT Purkinje cells at 5 to 9 weeks old (Figure 5). In TG mouse Purkinje cells, we frequently observed large cavities occupied in the soma. In addition, the TG Purkinje cells also have de-structured mitochondria. Compare to WT mice, TG mouse mitochondrial cristae was incomplete at 5 to 9 weeks old (Figure 6).

We also examined the axon of Purkinje cells. In the WT Purkinje cells, the compaction of myelin sheath was observed at 6 weeks old, however, the incompact myelin sheath of axons were still shown in the TG Purkinje cells until 9 weeks old (Figure 7).

Part 2. Evaluation of the therapeutic potential of SAHA and L-BMX on SCA17 transgenic mice

Long-term treatment of L-BMX or SAHA could not benefit to animals' performance on rotarod and locomotion

Both L-BMX and SAHA were identified to have beneficial effect on the cell survival and neurite outgrowth in our SCA3 cell lines (Yen, 2010). In addition, SAHA was reported to improve the motor function in R6/2 transgenic mice (Hockly et al., 2003). To explore whether these HDACi have potential in SCA17 treatment in vivo, the SCA17 mice administrated with L-BMX or SAHA started at the age of 4 weeks and the behavior tests were conducted scheduled as shown on the timeline (Figure 8). In order to assess the motor function of mice, we conducted rotarod test to record their latency on the rod. Our results showed that both HDACi compounds not only could not improve the mouse motor function but also deteriorate their behaviors in locomotion hyper-activity (Figure 9A) and rotarod performance (Figure 9B). TG mice treated with SAHA showed increased hyper-activity than vehicle-treated TG mice at the age of 16 weeks. In addition, WT littermates treated with either L-BMX or SAHA also decreased theirlatencyin rotarod tests after 16 weeks.

Mice treated with L-BMX or SAHA improved their performance in

the gait and beam tests

After administrated drugs for 16 weeks, TG mice showed better performance than TG control littermates in the beam test. TG mice treated with L-BMX spend less time to arrive the platform. In addition, TG mouse administrated with HDACi compounds improved the number of foot slips on the beam (Figure 10).

TG mice treated with HDACi compounds also improved their gait performance. The footprint analysis showed that L-BMX treated TG mice increased the length of forelimb steps of TG mice and SAHA treated TG mice increased the length of both forelimb and hindlimb steps (Figure 11).

L-BMX and SAHA could not rescue the phenotype of cerebellum atrophy

NeuN immunohistochemical staining was performed to investigate the morphology of cerebellum at the age of 20 weeks. Our results showed that HDACi compounds could not improve cerebellum atrophy of TG mice (Figure 12). In addition, calbindin immunofluorescent staining showed that HDACi compounds could not ameliorate the Purkinje cell loss (Figure 13A). Furthermore, western blot confirmed that HDACi compounds could not rescue the reduced expression level of calbindin (Figure 13B).

HDACi compounds rescued the astrocyte mediated gliosis

To investigate the effect of HDACi compounds on astrocyte

mediated gliosis, we used GFAP antibody to highlight astrocytes at the 20-week old mice. Our results showed that L-BMX administrated TG mice decreased the number of active astrocytes and also decreased the GFAP protein expression level compared to TG control littermates (Figure 14A). In addition, TG mice treated with SAHA also decreased the number of active astrocytes but did not alter the GFAP protein expression level (Figure 14B).

HDACi compounds rescued the Bergmann glia loss

S100 immunofluorescent staining was conducted to investigate the number of Bergmann glia at the 20-week old mice. Our results showed that TG mice treated with HDACi compounds could reduce the Bergmann glia loss (Figure 15).

HDACi compounds stimulated microglia activation

In order to investigate the inflammation in the cerebellum of TG mice at the age of 20 weeks, we used the Iba1 antibody against microglia for immunofluorescent staining. Our data show that mice treated with L-BMX or SAHA could stimulate microglia activation in the cerebella (Figure 16).

Discussion

Transgenic mice overexpression of mutant TBP in neuronal cells by the Purkinje cell specific promoter, L7/pcp2, which develop a progressive neurological phenotypes has been established in our lab as a SCA17 mouse model (Chang et al., 2011). Transgenic mice expressing TBP-109Q result in TBP loss of function, Purkinje cell loss, ataxia and motor incoordination, which have also been reported in SCA17 patients (Nakamura et al., 2001).

Previous study showed that knockdown of HDAC8 in neuroblastoma resulted in the inhibition of proliferation and differentiation (Yadav and Collman, 2009). In addition, the activated microglia could play protective function to help neuronal differentiation and cell survival in chronic inflammation environment (Jack et al., 2005). In addition, HDACi could restore the down-regulation of anti-oxidant capacity caused by inflammation and protect cell survival from insult of oxidative stress (Moisse and Strong, 2006). In accordance with our results, we observed the amelioration of astrocyte and microglia activation in SCA17 transgenic mouse cerebella after HDACi treatment. L-BMX and SAHA might inhibit neuron precursor cell differentiated to astrocyte and restore anti-oxidant capacity in this chronic inflammation environment.

The cerebellum can be divided into three parts: the vermis (medial cerebellum), the paravermis (intermediate cerebellum or pars intermedia) and the hemisphere (lateral cerebellum) (Apps and Garwicz, 2005). Developmental studies suggest that the development of the fundamental

cerebellar architecture begins the subdivision of five transverse zones in cerebellum (Ozol et al., 1999). A previous study showed that HSP25 expression pattern was restricted to the fifth transverse, posterior lobule, in the vermis (Apps and Hawkes, 2009). On the other hand, it was reported that mutant TBP could reduce the expression of HSP25 by tightly binding to nuclear factor-YA and affects its transcriptional activity (Friedman et al., 2007; Huang et al., 2011). These studies suggest that microglia activation could be induced at different lobes of cerebella. According to the different inflammation microenvironment, Purkinje cells in cerebellum might show degeneration of different degree. Therefore, we hypothesize that Purkinje cells, in different transverse zones and lobes, might suffer from different levels of stress at the early stage in SCA17 transgenic mice.

In several studies, dysfunction of Bergmann glia has been reported to be involved in the pathology of SCAs (Pavese et al., 2006; Morgan, 2009). Dysfunction of Bergmann glia caused Purkinje cells undergo non-cell-autonomous degeneration because of loss of the glutamate reuptake function and increasing of neurotoxicity in adulthood (Shiwaku et al., 2010). In previous study, Bergmann glia processes played a role of ensheathment in synapse development and formation (Lippman et al., 2008). Our results suggest HDACi treatment increased the number of Bergmann glia, which might further decrease the glutamate toxicity and enhance the synapses between Bergmann glia and Purkinje cells, resulted in the Purkinje cell loss on SCA17 transgenic mice at the age of 20 weeks. On the other hand, our early pathology analyses showed that the process

of Bergmann glia increased and astrocyte activation in transgenic mouse cerebella after the age of 4 weeks. This data implies that when Purkinje cells undergo degeneration in SCA17 transgenic mice, astrocyte and Bergmann glia are activated to rescue this situation. Therefore, in our pathology analyses, we observed that Bergmann glia and astrocyte were activated at the age of 4 weeks, earlier than the age when Purkinje cell loss.

Mitochondria play an important role in cellular functions including ATP generation and intracellular Ca^{2+} homeostasis. It is also response to the reactive oxygen species (ROS) formation and triggered the program cell death, apoptosis. Neurons critically rely on mitochondria for their highly active metabolism which demands high energy, (Keating, 2008). It was reported mitochondria are one of the primary targets in in inflammatory injury condition of many neurodegenerative diseases (Xie et al., 2004; Hunter et al., 2007; Samavati et al., 2008). From our TEM results, mitochondria dysfunction is also one of the phenomena in this SCA17 mouse model.

In cerebellar development studies, postnatal X-irradiation resulted in the large cavity in the dendrite of Purkinje cells in P30 amicroneuronal cerebellum (Altman, 1987; Altman and Bayer, 1997). This neurodegenerative phenomenon also could be observed in our SCA17 TG mouse model.

Compare to WT mice, our data indicated that Purkinje cell axons showed an incompact structure from the TEM experiments. This symptom indicates that synapses between Purkinje cells and deep

cerebellar nuclei of TG mice might be reduced. In addition, previous studies suggested that microglia may involve in removal of unwanted cells and synapse (Napoli and Neumann, 2009). Thus, the synapses between Purkinje cell and other organization, Bergmann glia, granule cell, basket cell, stellate cell, mossy fiber, climbing fiber and deep cerebellar nuclei (Altman and Bayer, 1997), might be influenced. It might explain why microglia were activated in the whole cerebellum, especially on the deep cerebellar nuclei and granule cell layer.

In our results, SCA17 transgenic mice treated with either the HDAC3 and HDAC8 inhibitor, L-BMX, or the pan-HDAC inhibitor, SAHA, could slightly improve the coordination and walking behavior of SCA17 transgenic mice.

Reference

Ajmone-Cat MA, Cacci E, Ragazzoni Y, Minghetti L, Biagioni S (2010) Pro-gliogenic effect of IL-1alpha in the differentiation of embryonic neural precursor cells in vitro. Journal of neurochemistry 113:1060-1072.

Alcendor RR, Gao S, Zhai P, Zablocki D, Holle E, Yu X, Tian B, Wagner T, Vatner SF, Sadoshima J (2007) Sirt1 regulates aging and resistance to oxidative stress in the heart. Circulation research 100:1512-1521.

Altman J, Bayer SA (1997) Development of the cerebellar system : in relation to its evolution, structure, and functions. Boca Raton: CRC Press.

Apps R, Garwicz M (2005) Anatomical and physiological foundations of cerebellar information processing. Nature reviews Neuroscience 6:297-311.

Apps R, Hawkes R (2009) Cerebellar cortical organization: a one-map hypothesis. Nature reviews Neuroscience 10:670-681.

Chang YC, Lin CY, Hsu CM, Lin HC, Chen YH, Lee-Chen GJ, Su MT, Ro LS, Chen CM, Hsieh-Li HM (2011) Neuroprotective effects of granulocyte-colony stimulating factor in a novel transgenic mouse model of SCA17. Journal of neurochemistry 118:288-303.

Daughters RS, Tuttle DL, Gao W, Ikeda Y, Moseley ML, Ebner TJ, Swanson MS, Ranum LP (2009) RNA gain-of-function in spinocerebellar ataxia type 8. PLoS genetics 5:e1000600.

Dohlinger S, Hauser TK, Borkert J, Luft AR, Schulz JB (2008) Magnetic

resonance imaging in spinocerebellar ataxias. Cerebellum 7:204-214.

Donmez G, Guarente L (2010) Aging and disease: connections to sirtuins. Aging cell 9:285-290.

Ferrante RJ, Kubilus JK, Lee J, Ryu H, Beesen A, Zucker B, Smith K, Kowall NW, Ratan RR, Luthi-Carter R, Hersch SM (2003) Histone deacetylase inhibition by sodium butyrate chemotherapy ameliorates the neurodegenerative phenotype in Huntington's disease mice. The Journal of neuroscience : the official journal of the Society for Neuroscience 23:9418-9427.

Fischer A, Sananbenesi F, Wang X, Dobbin M, Tsai LH (2007) Recovery of learning and memory is associated with chromatin remodelling. Nature 447:178-182.

Friedman MJ, Wang CE, Li XJ, Li S (2008) Polyglutamine expansion reduces the association of TATA-binding protein with DNA and induces DNA binding-independent neurotoxicity. The Journal of biological chemistry 283:8283-8290.

Friedman MJ, Shah AG, Fang ZH, Ward EG, Warren ST, Li S, Li XJ (2007) Polyglutamine domain modulates the TBP-TFIIB interaction: implications for its normal function and neurodegeneration. Nature neuroscience 10:1519-1528.

Guan JS, Haggarty SJ, Giacometti E, Dannenberg JH, Joseph N, Gao J, Nieland TJ, Zhou Y, Wang X, Mazitschek R, Bradner JE, DePinho RA, Jaenisch R, Tsai LH (2009) HDAC2 negatively regulates memory formation and synaptic plasticity. Nature 459:55-60.

Harding AE (1982) The clinical features and classification of the late onset autosomal dominant cerebellar ataxias. A study of 11 families, including descendants of the 'the Drew family of Walworth'. Brain : a journal of neurology 105:1-28.

Hockly E, Richon VM, Woodman B, Smith DL, Zhou X, Rosa E, Sathasivam K, Ghazi-Noori S, Mahal A, Lowden PA, Steffan JS, Marsh JL, Thompson LM, Lewis CM, Marks PA, Bates GP (2003) Suberoylanilide hydroxamic acid, a histone deacetylase inhibitor, ameliorates motor deficits in a mouse model of Huntington's disease. Proceedings of the National Academy of Sciences of the United States of America 100:2041-2046.

Huang S, Ling JJ, Yang S, Li XJ, Li S (2011) Neuronal expression of TATA box-binding protein containing expanded polyglutamine in knock-in mice reduces chaperone protein response by impairing the function of nuclear factor-Y transcription factor. Brain : a journal of neurology 134:1943-1958.

Inoue K, Tsuda M (2009) Microglia and neuropathic pain. Glia 57:1469-1479.

Jack C, Ruffini F, Bar-Or A, Antel JP (2005) Microglia and multiple sclerosis. Journal of neuroscience research 81:363-373.

Kaindl AM, Favrais G, Gressens P (2009) Molecular mechanisms involved in injury to the preterm brain. Journal of child neurology 24:1112-1118.

Kim HJ, Leeds P, Chuang DM (2009) The HDAC inhibitor, sodium butyrate, stimulates neurogenesis in the ischemic brain. Journal of

neurochemistry 110:1226-1240.

Koide R, Kobayashi S, Shimohata T, Ikeuchi T, Maruyama M, Saito M, Yamada M, Takahashi H, Tsuji S (1999) A neurological disease caused by an expanded CAG trinucleotide repeat in the TATA-binding protein gene: a new polyglutamine disease? Human molecular genetics 8:2047-2053.

Lambertsen KL, Clausen BH, Babcock AA, Gregersen R, Fenger C, Nielsen HH, Haugaard LS, Wirenfeldt M, Nielsen M, Dagnaes-Hansen F, Bluethmann H, Faergeman NJ, Meldgaard M, Deierborg T, Finsen B (2009) Microglia protect neurons against ischemia by synthesis of tumor necrosis factor. The Journal of neuroscience : the official journal of the Society for Neuroscience 29:1319-1330.

Lin MT, Beal MF (2006) Mitochondrial dysfunction and oxidative stress in neurodegenerative diseases. Nature 443:787-795.

Manto MU (2005) The wide spectrum of spinocerebellar ataxias (SCAs). Cerebellum 4:2-6.

Marks P, Rifkind RA, Richon VM, Breslow R, Miller T, Kelly WK (2001) Histone deacetylases and cancer: causes and therapies. Nature reviews Cancer 1:194-202.

Marks PA, Dokmanovic M (2005) Histone deacetylase inhibitors: discovery and development as anticancer agents. Expert opinion on investigational drugs 14:1497-1511.

Michishita E, Park JY, Burneskis JM, Barrett JC, Horikawa I (2005) Evolutionarily conserved and nonconserved cellular localizations

and functions of human SIRT proteins. Molecular biology of the cell 16:4623-4635.

Moisse K, Strong MJ (2006) Innate immunity in amyotrophic lateral sclerosis. Biochimica et biophysica acta 1762:1083-1093.

Morgan D (2009) The role of microglia in antibody-mediated clearance of amyloid-beta from the brain. CNS & neurological disorders drug targets 8:7-15.

Nakamura K, Jeong SY, Uchihara T, Anno M, Nagashima K, Nagashima T, Ikeda S, Tsuji S, Kanazawa I (2001) SCA17, a novel autosomal dominant cerebellar ataxia caused by an expanded polyglutamine in TATA-binding protein. Human molecular genetics 10:1441-1448.

Napoli I, Neumann H (2009) Microglial clearance function in health and disease. Neuroscience 158:1030-1038.

Ozol K, Hayden JM, Oberdick J, Hawkes R (1999) Transverse zones in the vermis of the mouse cerebellum. The Journal of comparative neurology 412:95-111.

Pavese N, Gerhard A, Tai YF, Ho AK, Turkheimer F, Barker RA, Brooks DJ, Piccini P (2006) Microglial activation correlates with severity in Huntington disease: a clinical and PET study. Neurology 66:1638-1643.

Reid SJ, Rees MI, van Roon-Mom WM, Jones AL, MacDonald ME, Sutherland G, During MJ, Faull RL, Owen MJ, Dragunow M, Snell RG (2003) Molecular investigation of TBP allele length: a SCA17 cellular model and population study. Neurobiology of disease

13:37-45.

Renthal W, Maze I, Krishnan V, Covington HE, 3rd, Xiao G, Kumar A, Russo SJ, Graham A, Tsankova N, Kippin TE, Kerstetter KA, Neve RL, Haggarty SJ, McKinsey TA, Bassel-Duby R, Olson EN, Nestler EJ (2007) Histone deacetylase 5 epigenetically controls behavioral adaptations to chronic emotional stimuli. Neuron 56:517-529.

Ryu H, Smith K, Camelo SI, Carreras I, Lee J, Iglesias AH, Dangond F, Cormier KA, Cudkowicz ME, Brown RH, Jr., Ferrante RJ (2005) Sodium phenylbutyrate prolongs survival and regulates expression of anti-apoptotic genes in transgenic amyotrophic lateral sclerosis mice. Journal of neurochemistry 93:1087-1098.

Savchenko VL, McKanna JA, Nikonenko IR, Skibo GG (2000) Microglia and astrocytes in the adult rat brain: comparative immunocytochemical analysis demonstrates the efficacy of lipocortin 1 immunoreactivity. Neuroscience 96:195-203.

Schaffar G, Breuer P, Boteva R, Behrends C, Tzvetkov N, Strippel N, Sakahira H, Siegers K, Hayer-Hartl M, Hartl FU (2004) Cellular toxicity of polyglutamine expansion proteins: mechanism of transcription factor deactivation. Molecular cell 15:95-105.

Shah AG, Friedman MJ, Huang S, Roberts M, Li XJ, Li S (2009) Transcriptional dysregulation of TrkA associates with neurodegeneration in spinocerebellar ataxia type 17. Human molecular genetics 18:4141-4152.

Shiwaku H, Yoshimura N, Tamura T, Sone M, Ogishima S, Watase K,

Tagawa K, Okazawa H (2010) Suppression of the novel ER protein Maxer by mutant ataxin-1 in Bergman glia contributes to non-cell-autonomous toxicity. The EMBO journal 29:2446-2460.

Steffan JS, Bodai L, Pallos J, Poelman M, McCampbell A, Apostol BL, Kazantsev A, Schmidt E, Zhu YZ, Greenwald M, Kurokawa R, Housman DE, Jackson GR, Marsh JL, Thompson LM (2001) Histone deacetylase inhibitors arrest polyglutamine-dependent neurodegeneration in Drosophila. Nature 413:739-743.

Stevanin G, Brice A (2008) Spinocerebellar ataxia 17 (SCA17) and Huntington's disease-like 4 (HDL4). Cerebellum 7:170-178.

Trottier Y, Lutz Y, Stevanin G, Imbert G, Devys D, Cancel G, Saudou F, Weber C, David G, Tora L, et al. (1995) Polyglutamine expansion as a pathological epitope in Huntington's disease and four dominant cerebellar ataxias. Nature 378:403-406.

Tsai LK, Tsai MS, Ting CH, Li H (2008) Multiple therapeutic effects of valproic acid in spinal muscular atrophy model mice. J Mol Med (Berl) 86:1243-1254.

Tsankova NM, Berton O, Renthal W, Kumar A, Neve RL, Nestler EJ (2006) Sustained hippocampal chromatin regulation in a mouse model of depression and antidepressant action. Nature neuroscience 9:519-525.

van Roon-Mom WM, Reid SJ, Faull RL, Snell RG (2005) TATA-binding protein in neurodegenerative disease. Neuroscience 133:863-872.

Voelter-Mahlknecht S, Ho AD, Mahlknecht U (2005) Chromosomal organization and localization of the novel class IV human histone

deacetylase 11 gene. International journal of molecular medicine 16:589-598.

Weinstein JR, Koerner IP, Moller T (2010) Microglia in ischemic brain injury. Future neurology 5:227-246.

Whaley NR, Fujioka S, Wszolek ZK (2011) Autosomal dominant cerebellar ataxia type I: A review of the phenotypic and genotypic characteristics. Orphanet journal of rare diseases 6:33.

Yadav A, Collman RG (2009) CNS inflammation and macrophage/microglial biology associated with HIV-1 infection. Journal of neuroimmune pharmacology : the official journal of the Society on NeuroImmune Pharmacology 4:430-447.

Yang XJ, Seto E (2008) The Rpd3/Hda1 family of lysine deacetylases: from bacteria and yeast to mice and men. Nature reviews Molecular cell biology 9:206-218.

Zoghbi HY, Orr HT (2000) Glutamine repeats and neurodegeneration. Annual review of neuroscience 23:217-247.

Zuhlke C, Hellenbroich Y, Dalski A, Kononowa N, Hagenah J, Vieregge P, Riess O, Klein C, Schwinger E (2001) Different types of repeat expansion in the TATA-binding protein gene are associated with a new form of inherited ataxia. European journal of human genetics : EJHG 9:160-164.

Table 1. Information of the primary antibodies

Detection	Host species	Titer	Source	Goal
NeuN	Mouse-monoclonal	1:1000	Millipore	Total neuron
Calbindin	Rabbit-polyclonal	1:1000	Sigma	Purkinje cell marker
GFAP	Mouse-monoclonal	1:500	Millipore	Astrocyte marker
S100	Mouse-monoclonal	1:500	Sigma	Bergmann glia marker
Iba1	Rabbit-polyclonal	1:500	Wako	Microglia marker

Table 2

Summary of part 1

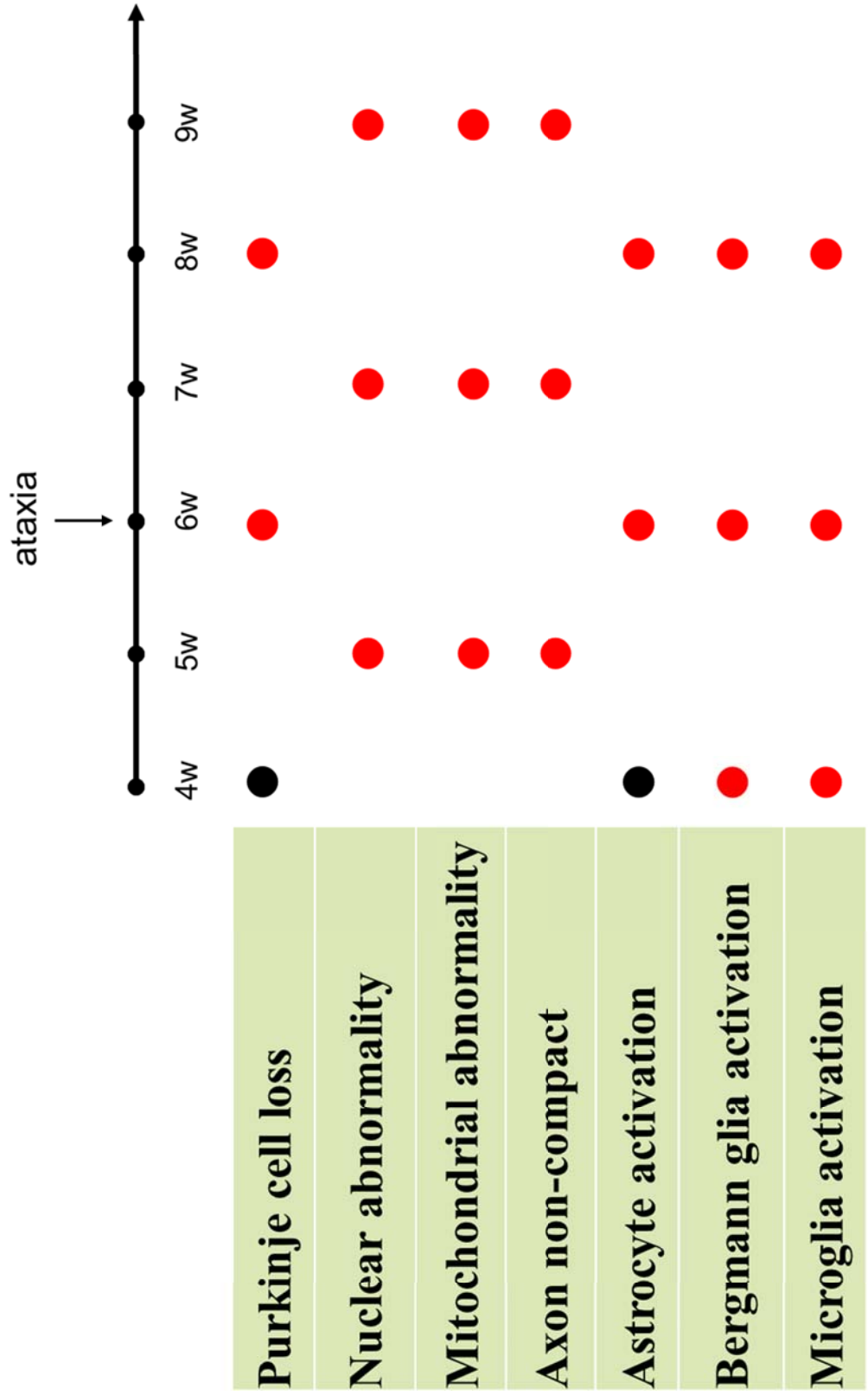

Table 3

Summary of part 2

	Compare to TG DMSO	
	TG L-BMX	TG SAHA
Locomotor hyperactivity	—	↑
Rotarod performance	—	—
Beam test performance	↓	—
Footprint performance	↑	↑
Cerebellum atrophy	—	—
Purkinje cell loss	—	—
Gliosis	↓	—
Bergmann glia loss	↓	—
Microglia activation	↑	↑

Figure

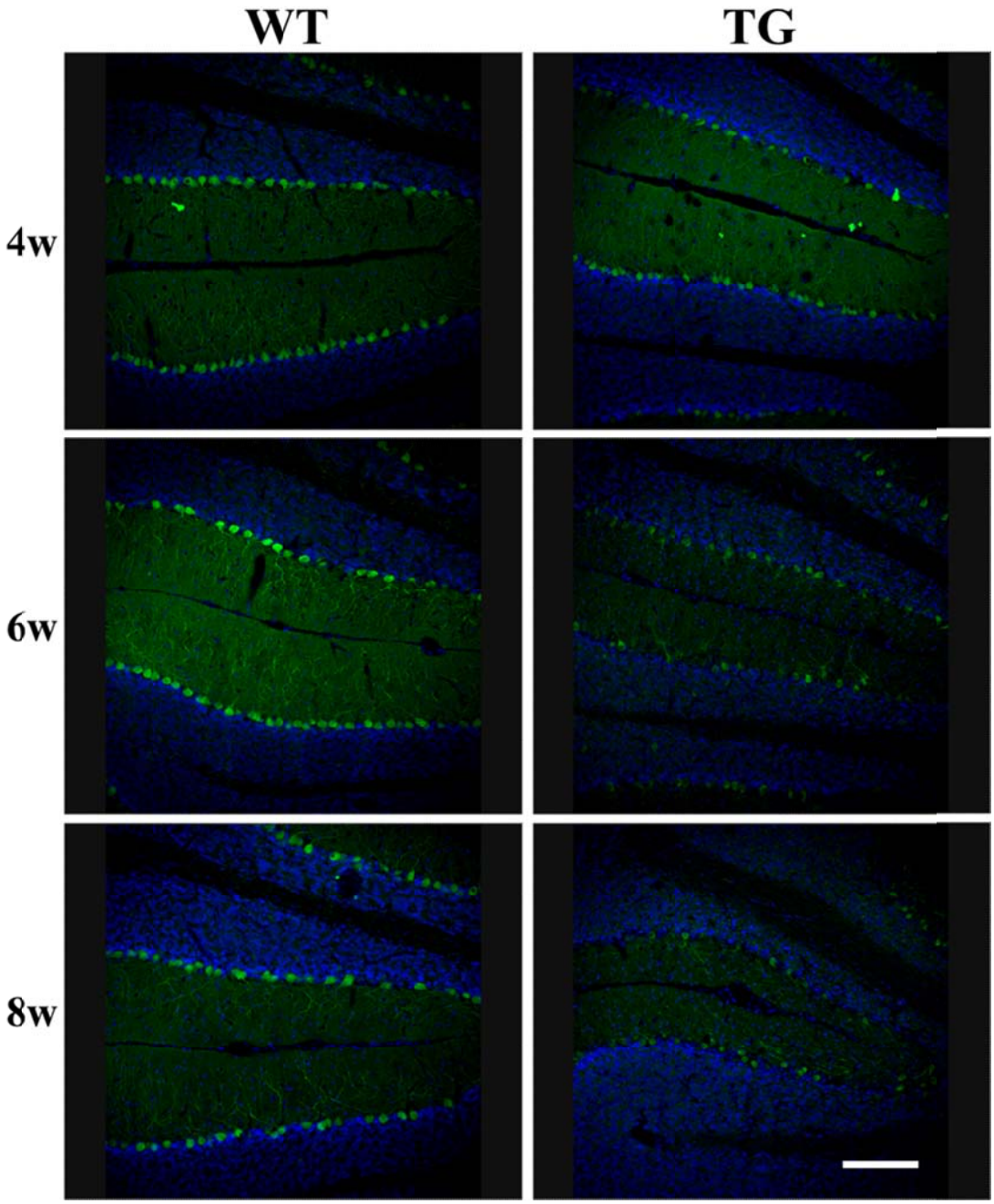

Figure 1. Purkinje cell analysis on hTBP-109Q transgenic mouse cerebella.

Cerebellar sagittal-sections were stained for nuclei with DAPI (blue) and for Purkinje cell (calbindin, green).Representative results of immunohistochemistry staining of calbindin of mouse cerebella. No significant Purkinje cell loses was identified in cerebellum of TG mice at 4-week old. However, a severe Purkinje cell loss was observed after 6 weeks old in TG mouse cerebella. n =3, scale bar = 150 μm.

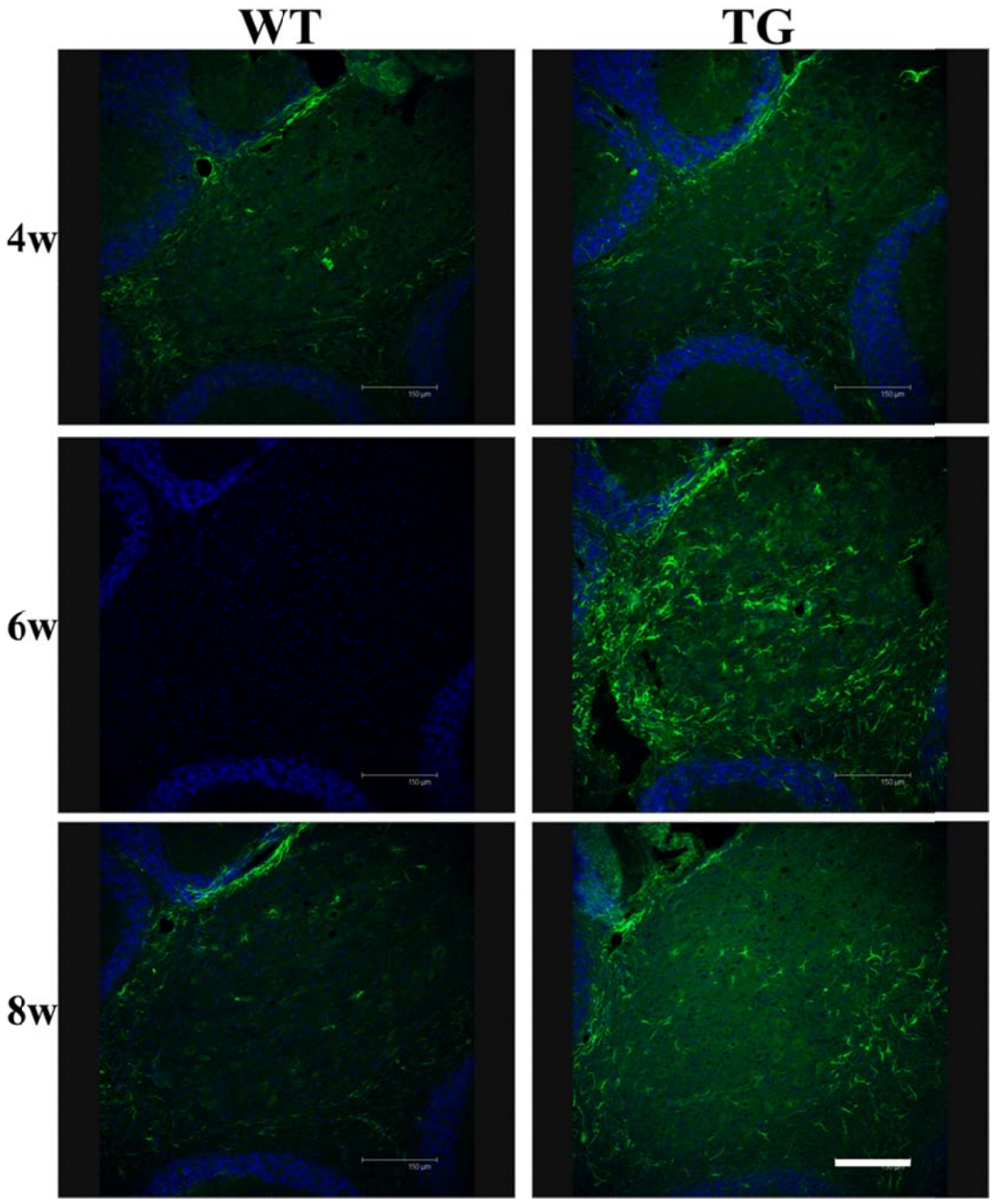
WT
TG
4w
6w
8w

Figure 2. Astrocyte activation in hTBP-109Q transgenic mouse cerebella.

Cerebellum sagittal-sections were stained for nuclei with DAPI (blue) and for astrocyte (GFAP, green).Representative results of GFAP immunofluorescent staining on mouse cerebella. Astrocyte activation was detected at the age of 6 week old transgenic mice. n =3, scale bar = 150 μm.

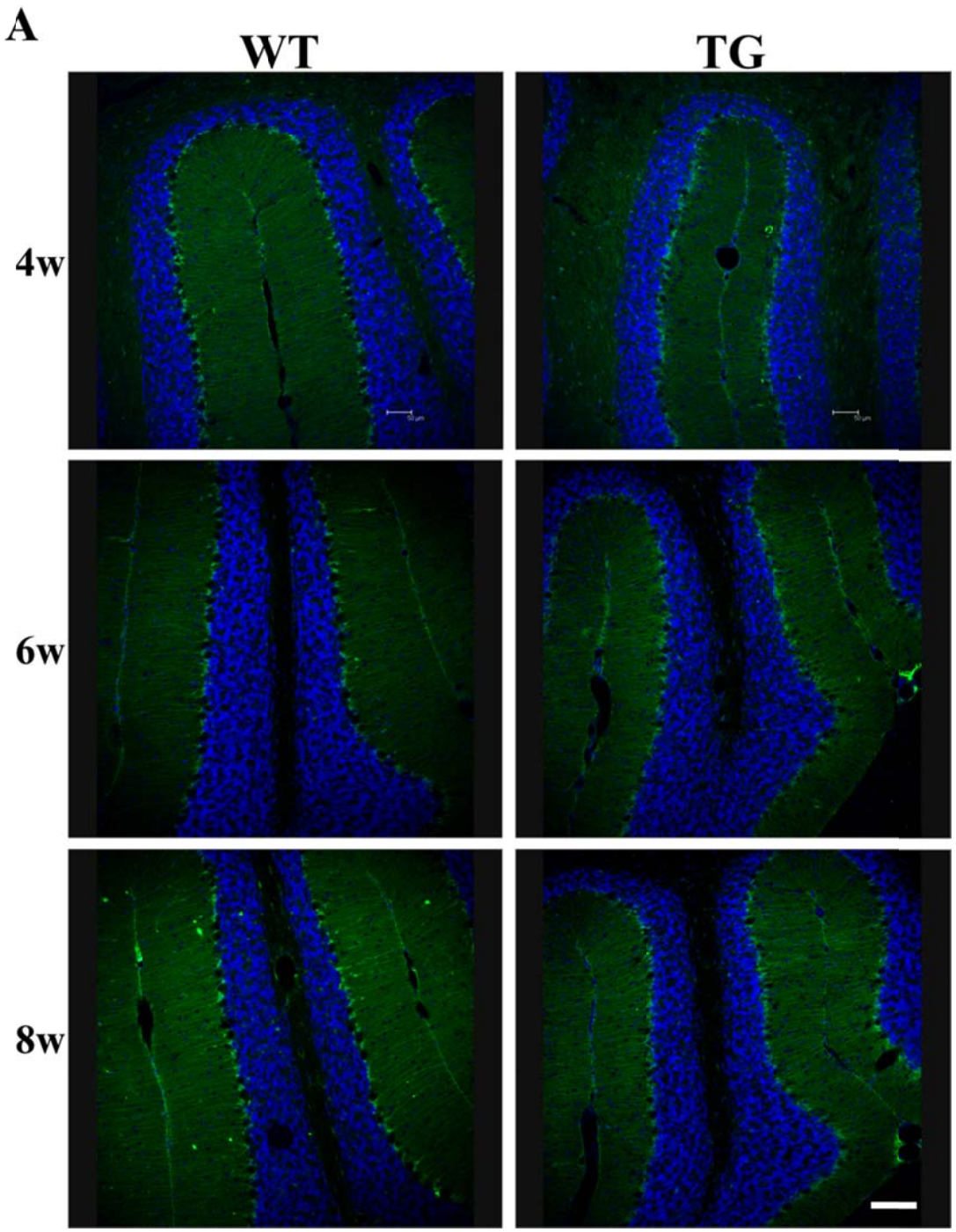

Figure 3.Bergmann gliosis in hTBP-109Q transgenic mouse cerebella.

Cerebellar sagittal-sections were stained for nuclei (DAPI, blue) and Bergmann glia (S100, green). (A) Immunofluorescent staining of mouse cerebella with Bergmann glia marker S100. (B) The S100 fluorescent signal in Purkinje cell layer of TG mouse cerebellum showed processing of Bergmann glia surrounding the Purkinje neurons was increased.

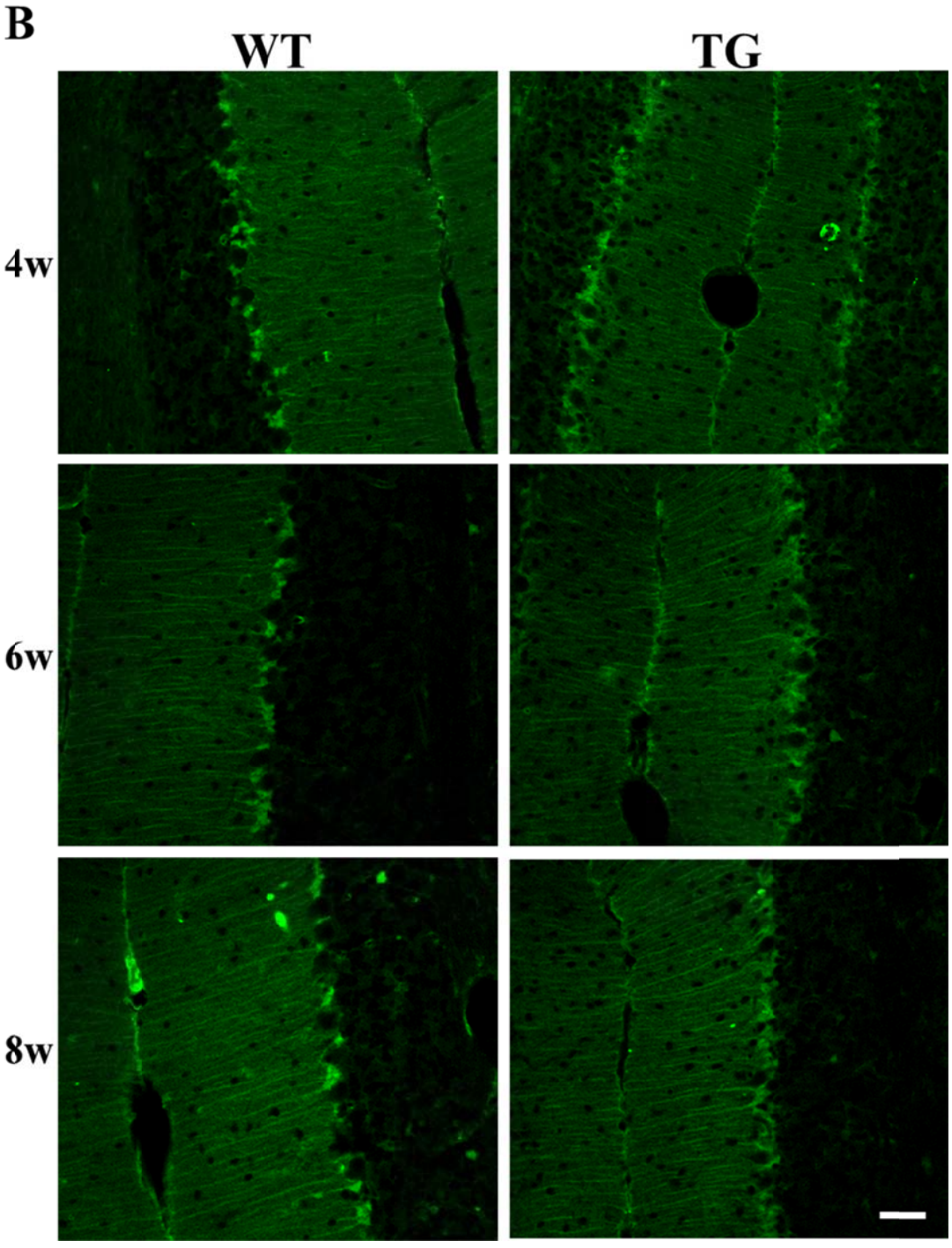
B
WT
TG
4w
6w
8w

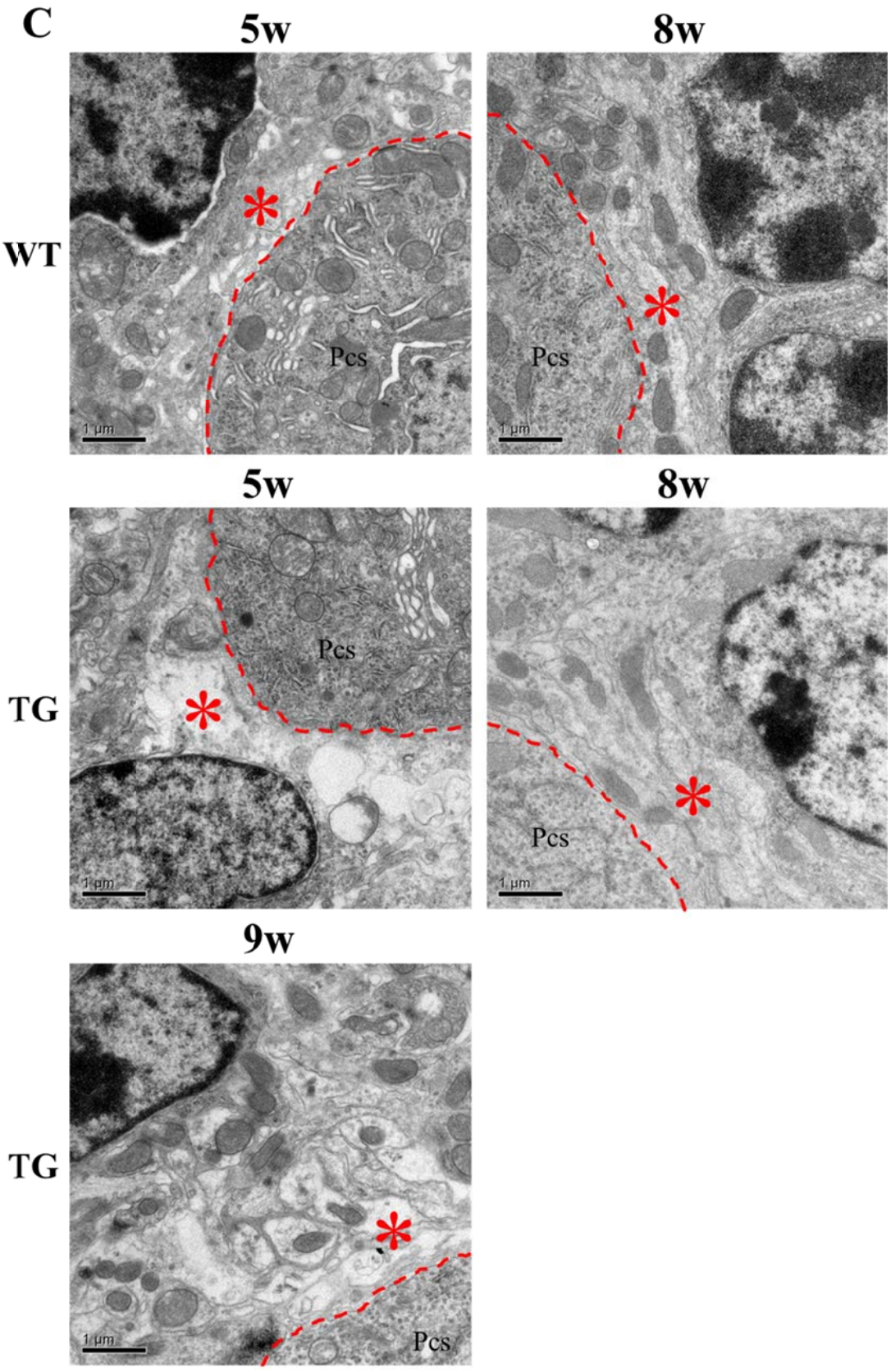
C
5w
8w
WT
Pcs
Pcs
1 μm
1 μm
5w
8w
TG
Pcs
Pcs
1 μm
1 μm
9w
TG
Pcs
1 μm

(C) TEM analyses also indicated that the numbers of Bergmann glia process (asterisk) in TG mice were increased. n =3, scale bar = 80 μm (A), 80 μm (B), 1 μm (C).

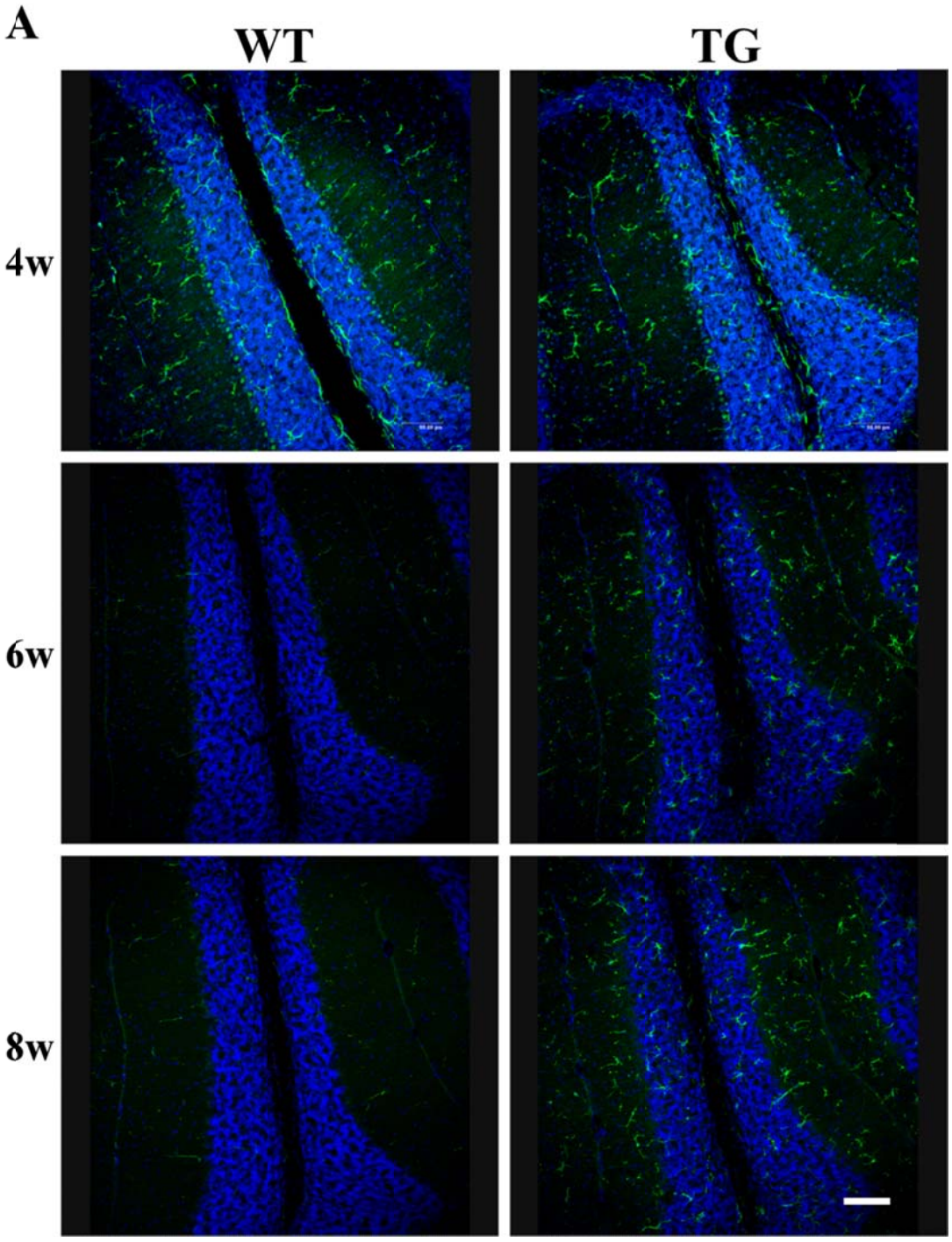

Figure 4.Neuroinflammation in hTBP-109Q transgenic mouse cerebella.

Cerebellar sagittal-sections were stained for nuclei (DAPI, blue) and microglia (Iba1, green). (A) Immunofluorescent staining of mouse cerebella with microglia marker Iba1. TG mice showed microglia activation in their cerebella at the ages of 4 to 8-weeks old.

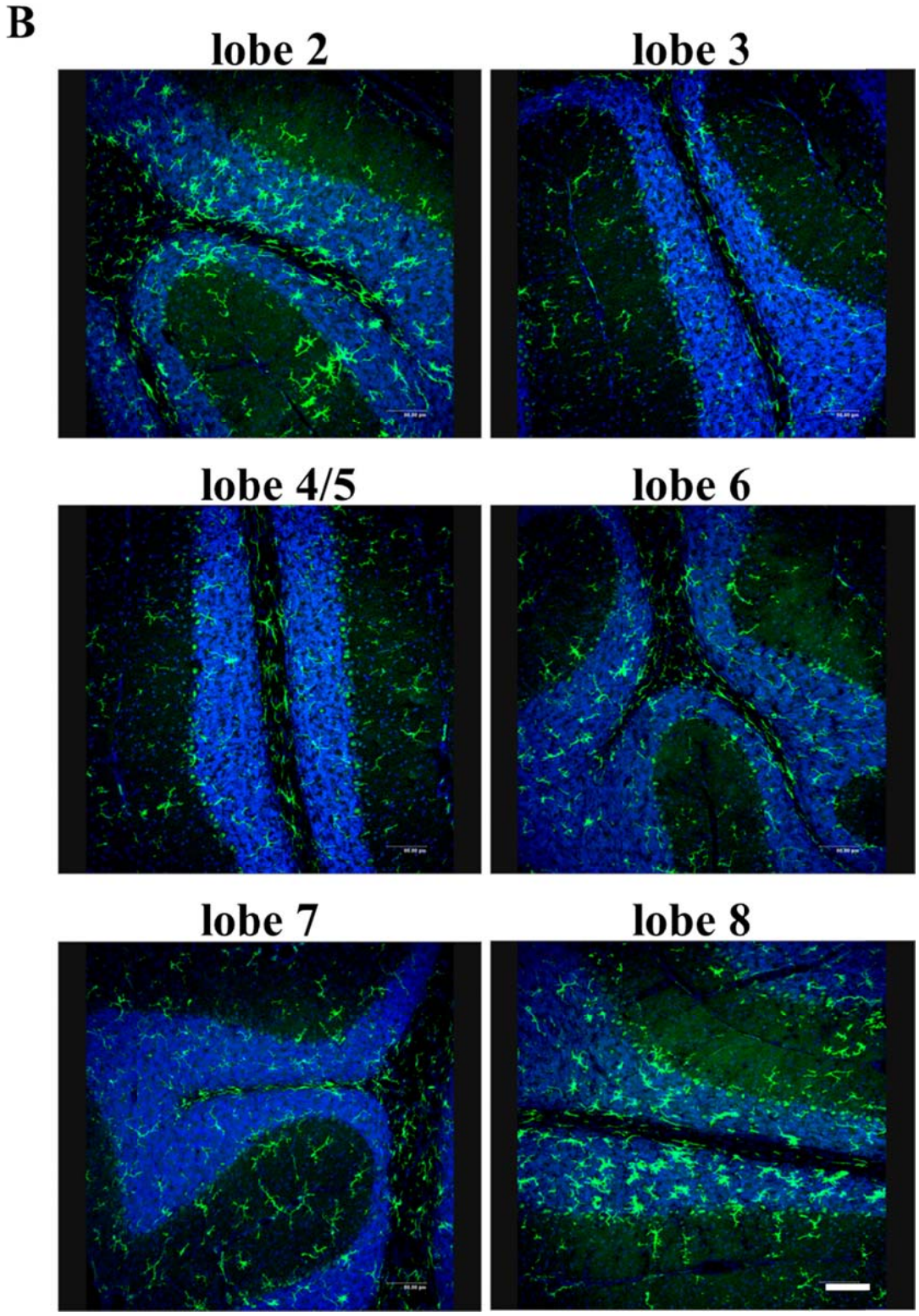

(B) More activated microglia were presented in lobes 2 and 8 than lobes 3-7 at 4 weeks old TG mice. n =3, scale bar = 80 μm.

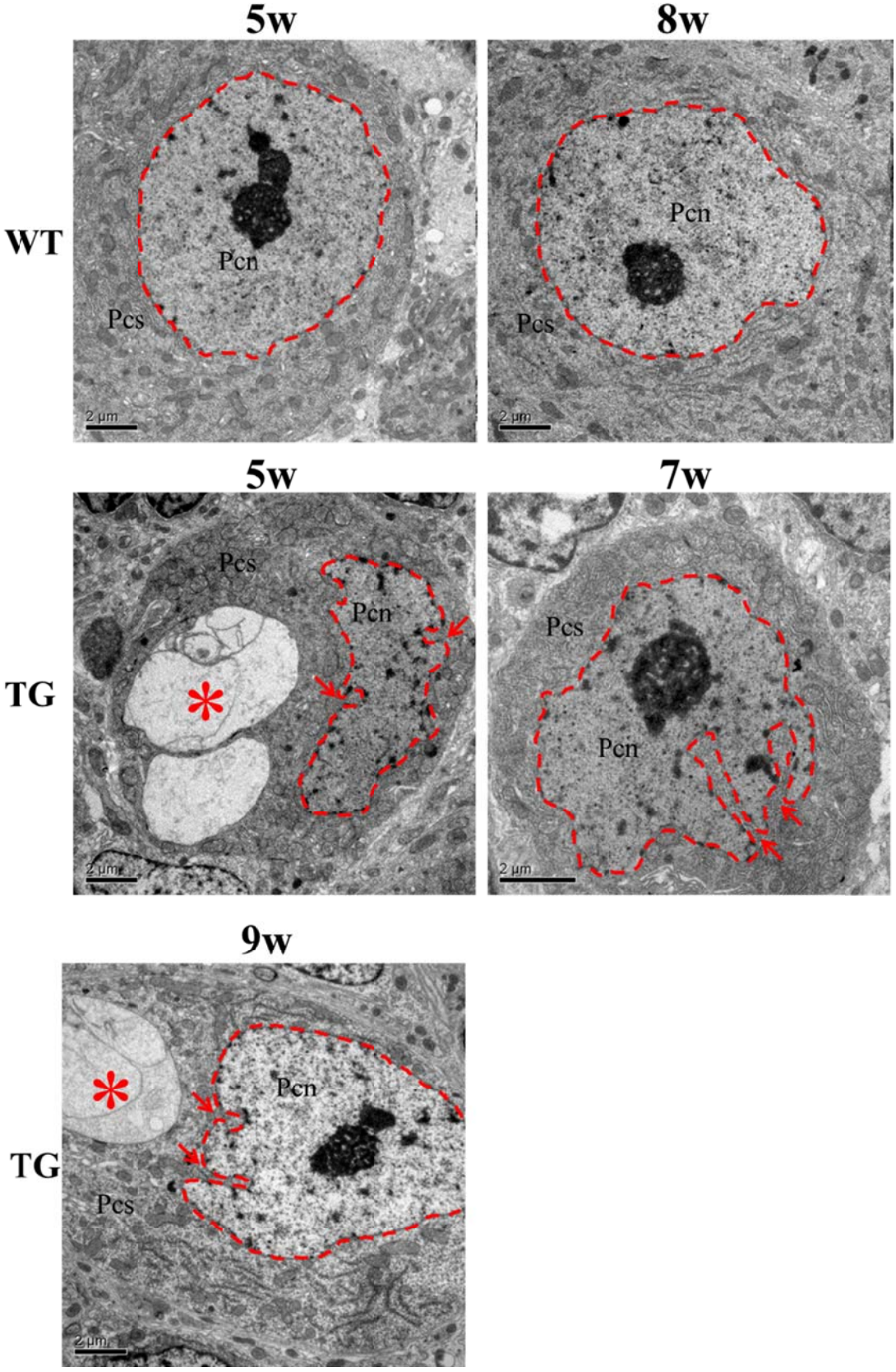
5w
8w
WT
Pcn
Pcs
2 μm
Pcn
Pcs
2 μm
5w
7w
TG
Pcs
Pcn
*
2 μm
Pcs
Pcn
2 μm
9w
TG
*
Pcn
Pcs
2 μm

Figure 5. Abnormal features in TG mouse Purkinje cells.

Compare to WT mice, TG mice showed irregular nuclei morphology (arrows) in the Purkinje cells at the age of 5 to 9 weeks old. These abnormal Purkinje cells usually accompany large cavities (asterisk) in the soma. Scale bar = 2 μm. Pcn, Purkinje cell nucleus; Pcs, Purkinje cell soma.

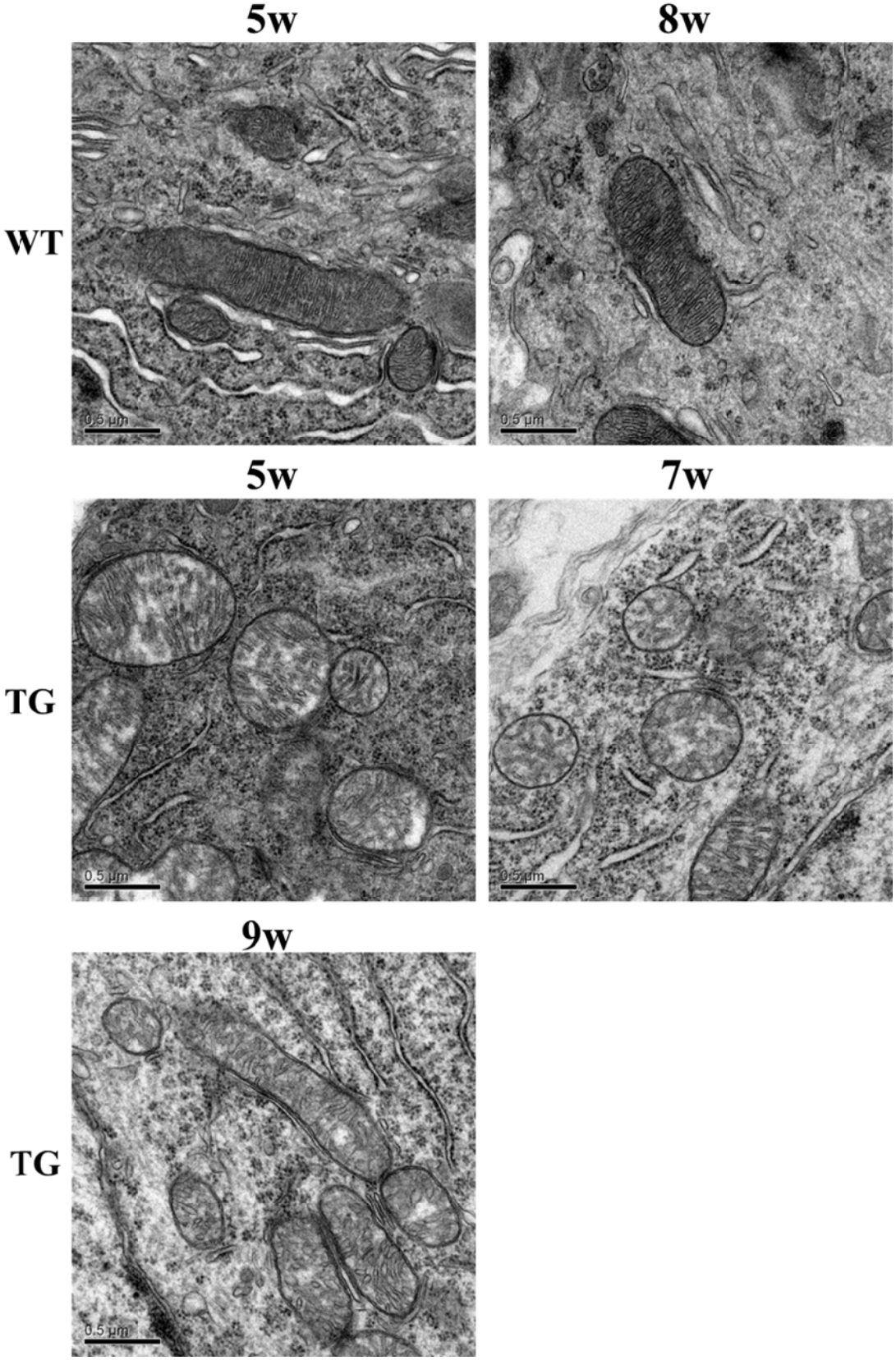
5w
8w
WT
0.5 μm
0.5 μm
5w
7w
TG
0.5 μm
0.5 μm
9w
TG
0.5 μm

Figure 6. Abnormal mitochondrial structure in TG mouse Purkinje cells.

Compare to WT mice, mitochondrial morphology of Purkinje cells in TG mice showed broken cristae at the age of 5 to 9 weeks old. Scale bar = 0.5 μm.

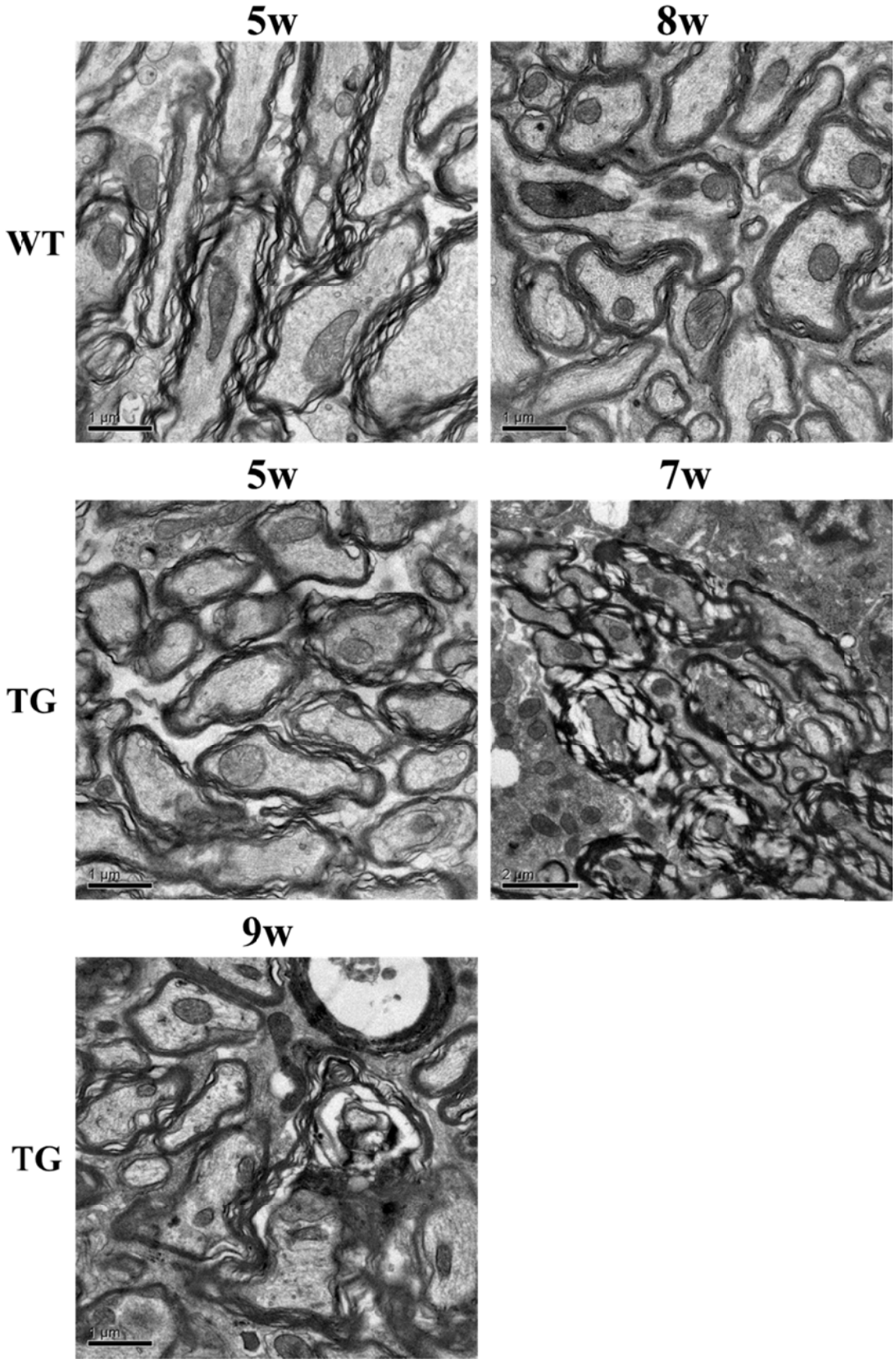
5w
8w
WT
1 μm
1 μm
5w
7w
TG
1 μm
2 μm
9w
TG
1 μm

Figure 7. Abnormal compaction of axons in TG mouse Purkinje cells. At the age of 5 weeks old, the axon of Purkinje cell displayed an incompact myelin sheath in both WT and TG mice. This phenomenon was disappeared at the age of 8 weeks old WT mice. However, mitochondria of TG mice still showed incompact myelin sheath at the age of 9 weeks old. Scale bar = 0.5 μm.

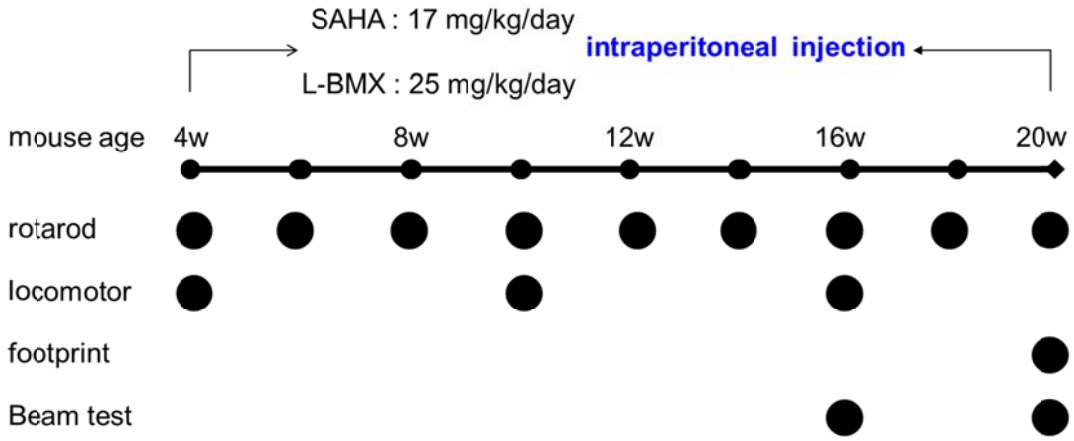
SAHA : 17 mg/kg/day
intraperitoneal injection
L-BMX : 25 mg/kg/day
mouse age
4w
8w
12w
16w
20w
rotarod
locomotor
footprint
Beam test

Figure 8. Timeline of HDACi compounds treatment and behavior tests.

Mice were administrated intraperitoneal injection daily with drugs from the age of 4 weeks to 20 weeks. Behavior tests were conducted every 2 weeks for rotarod tests and every 6 weeks for locomotor analyses. Footprint analyses were performed at the age of 20 weeks, and beam tests were performed at the age of 16 weeks and 20 weeks.

A. locomotor

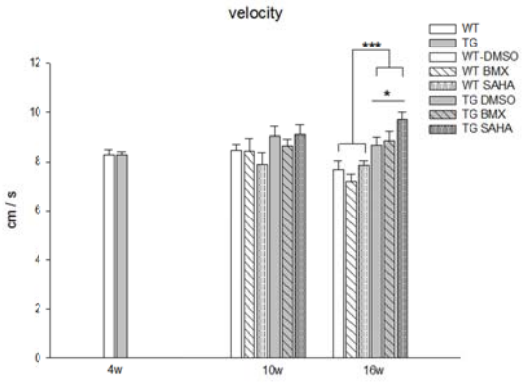

B. rotarod

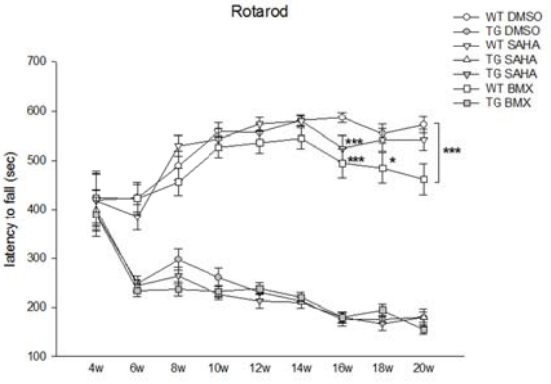

Figure 9.Locomotion and rotarod performance of animals during the treatment of L-BMX or SAHA.

(A) Locomotor activity of mice. TG mice treated with SAHA showed higher motor activity than TG control littermates. (B) Rotarod performance of mice. HDACi compound treatment could not increase the performance of TG groups. At the mouse age of 16 weeks, WT mice treated with L-BMX or SAHA showed decrease of latency. n $\geqq$13. Values represent means ± SE. *, $p< 0.05$, ***, $p< 0.001$. Statistics were conducted with two-factor ANOVA, and post-hoc analysis Scheffe test.

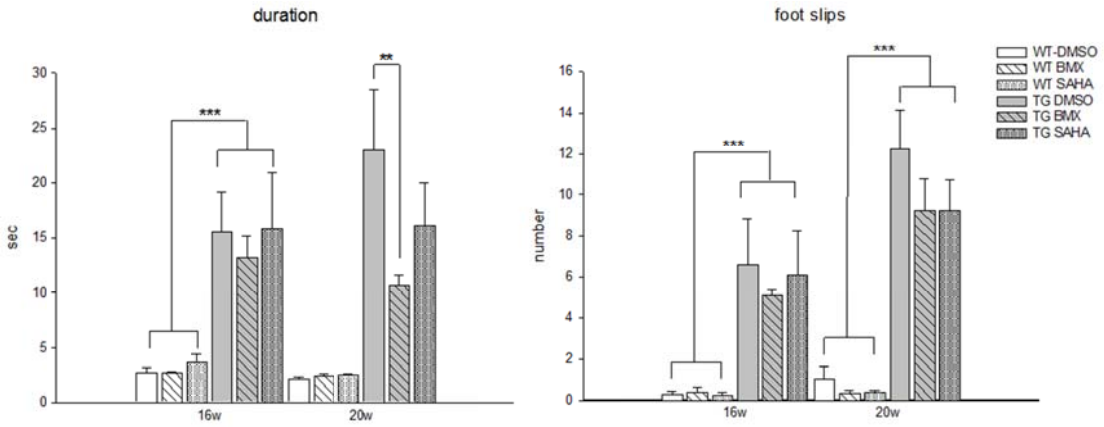
duration
sec
30
25
20
15
10
5
0
***
**
16w
20w
foot slips
number
16
14
12
10
8
6
4
2
0
***
***
16w
20w
WT-DMSO
WT BMX
WT SAHA
TG DMSO
TG BMX
TG SAHA

Figure 10. Mouse performance in beam tests after treated with L-BMX or SAHA.

(A) The duration on the beam was not altered by the treatment at 16 week old mice. TG mice improved the motor coordination after treated with L-BMX at the age of 20 weeks. (B) TG mice treated with L-BMX or SAHA decreased their number of foot slips on the beam. n $\geqq$13. Values represent means ± SE. **, p< 0.01, ***, *p*< 0.001. Statistics were conducted with two-factor ANOVA, and post-hoc analysis Scheffe test.

A

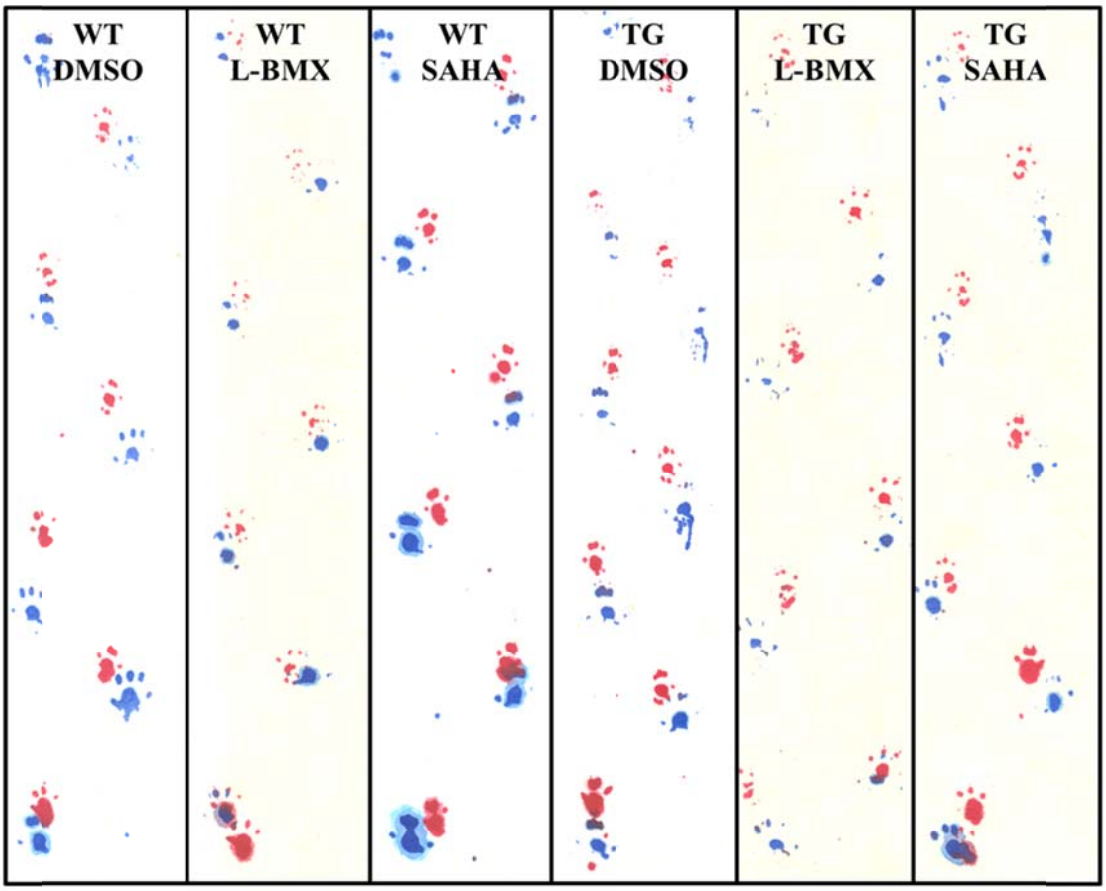
WT
DMSO
WT
L-BMX
WT
SAHA
TG
DMSO
TG
L-BMX
TG
SAHA

B

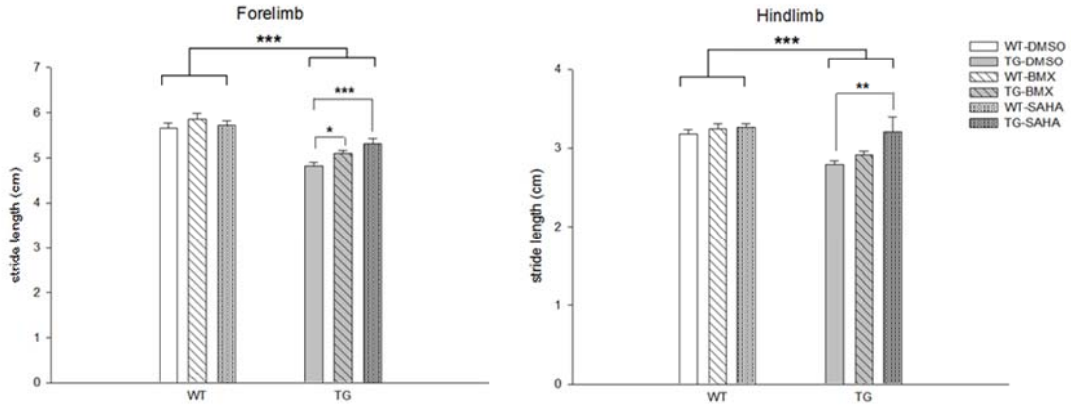
Forelimb
***
***
*
stride length (cm)
0
1
2
3
4
5
6
7
WT
TG
Hindlimb
***
**
stride length (cm)
0
1
2
3
4
WT
TG
WT-DMSO
TG-DMSO
WT-BMX
TG-BMX
WT-SAHA
TG-SAHA

Figure 11. Mouse performance in gait analyses after treated with L-BMX or SAHA.

(A) Represented results of gait analysis of mice. (B) Quantification of forelimb and hindlimb distance. TG mice increased the step length of forelimb after treated with L-BMX or SAHA. TG mice treated with SAHA also increased their length of hindlimb steps. n $\geqq$13. Values represent means ± SE. *, $p< 0.05$, **, $p< 0.01$, ***, $p< 0.001$. Statistics were conducted with two-factor ANOVA, and post-hoc analysis Scheffe test.

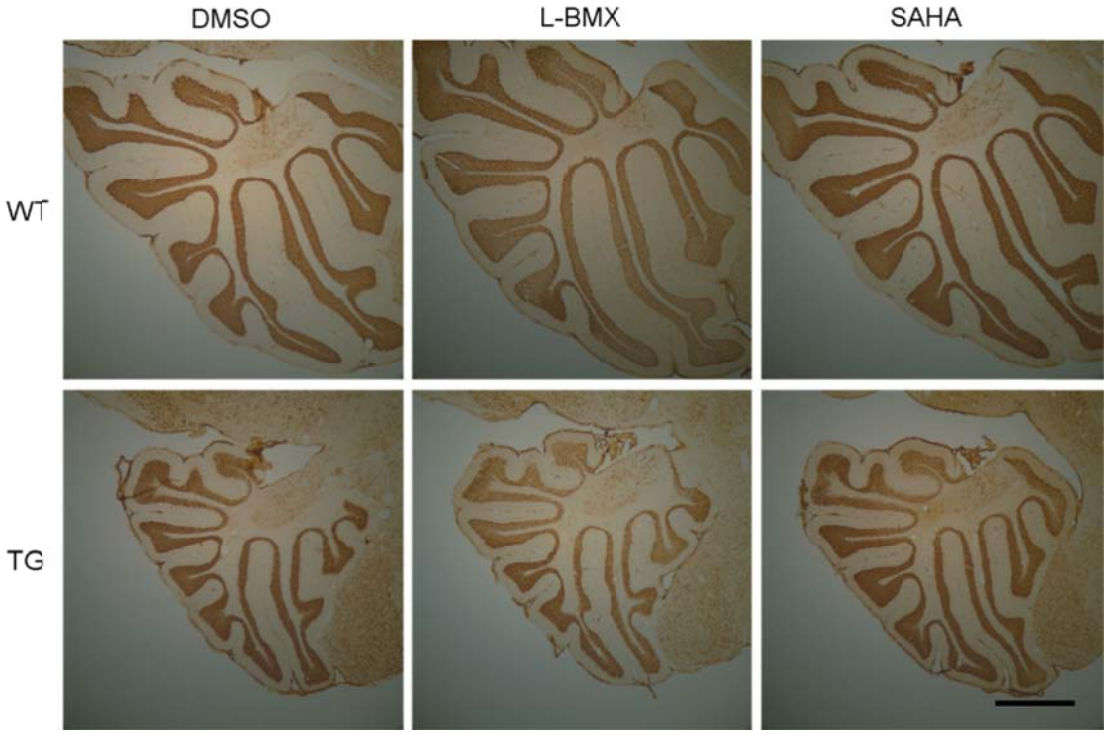
DMSO
L-BMX
SAHA
WT
TG

Figure 12.Cerebellar morphology of mice after L-BMX or SAHA treatment.

Cerebellar morphology was identified by immunohistochemistry staining of NeuN. TG mice treated with HDACi compounds could not rescue their cerebellum atrophy. Scale bar = 500 μm.

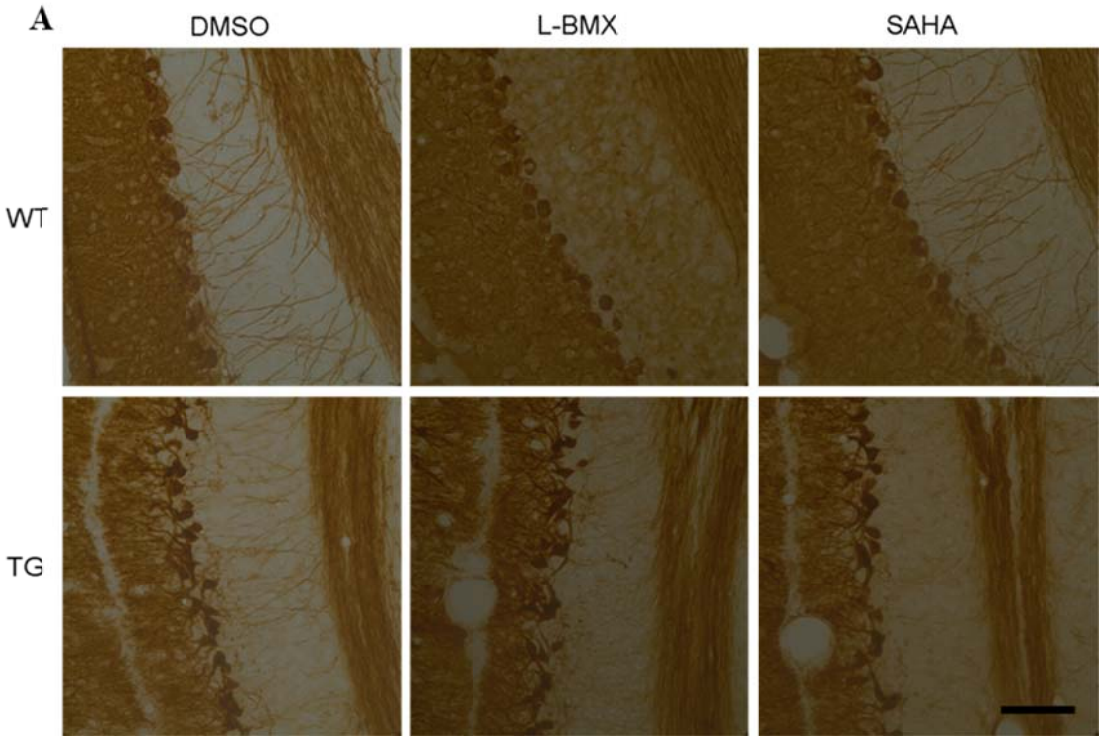
A
DMSO
L-BMX
SAHA
WT
TG

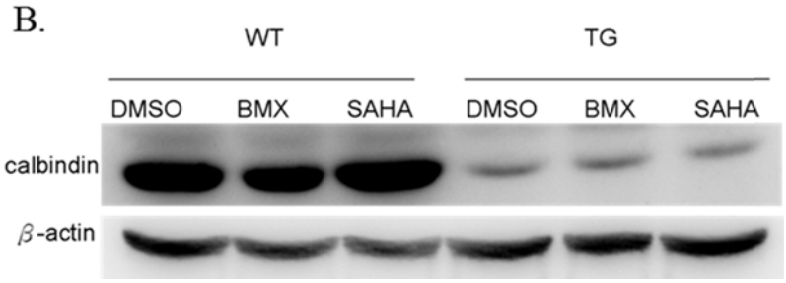
B.
WT
TG
DMSO
BMX
SAHA
DMSO
BMX
SAHA
calbindin
β-actin

Figure 13. Pathology analyses of mice after administration of L-BMX or SAHA.

(A) Representative results of immunohistochemistry staining of calbindin of mouse cerebellum. No amelioration in Purkinje cell loses was identified in cerebella of TG mice after treated with L-BMX or SAHA. (B) Western blot analyses of 20 week-old mouse cerebellum with calbindin antibody. TG mice treated with these two HDACi compounds could not restore their expression level of calbindin in the cerebella. Scale bar = 50 μm.

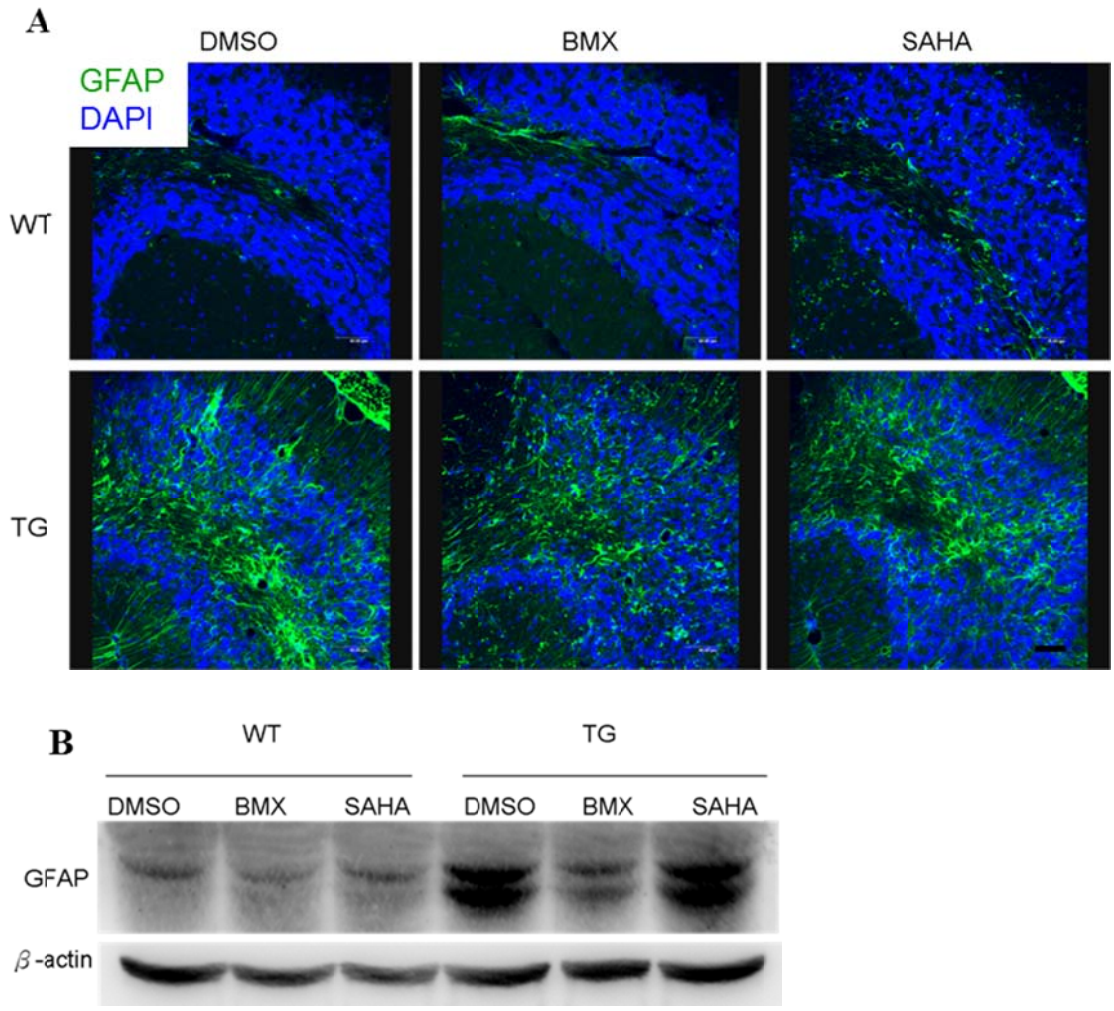
A
DMSO
BMX
SAHA
GFAP
DAPI
WT
TG
B
WT
TG
DMSO
BMX
SAHA
DMSO
BMX
SAHA
GFAP
β-actin

Figure 14. Gliosis level of cerebellum after mice treated with HDACi compounds.

Cerebellar sagittal-sections were stained for nuclei with DAPI (blue) and for astrocyte (GFAP, green). (A) Representative results of immunofluorescent staining of GFAP of mouse cerebella. TG mice treated with L-BMX or SAHA decreased the number of active astrocytes in their cerebella. (B) Western blot analyses of 20 week-old mouse cerebellum with GFAP antibody. Down regulation of GFAP expression was identified in TG mice treated with L-BMX. Scale bar = 40 μm.

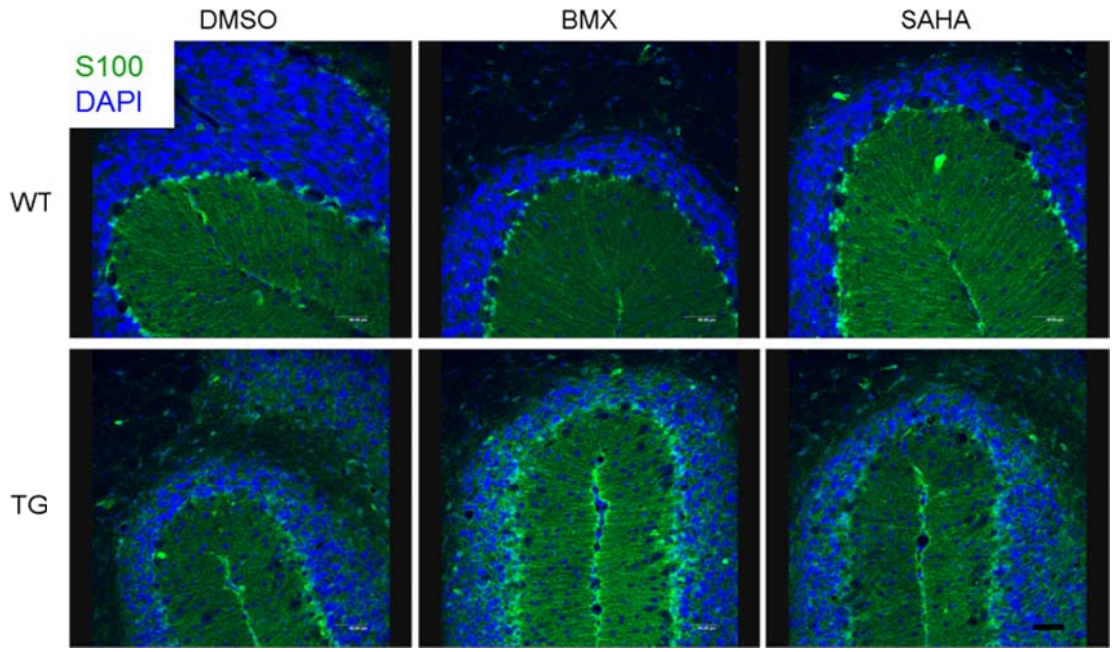
DMSO
BMX
SAHA
S100
DAPI
WT
TG

Figure 15.Bergmann glia characterization in animals administrated with L-BMX or SAHA.

Cerebellar sagittal-sections were stained for nuclei with DAPI (blue) and for Bergmann glia (S100, green).Immunofluorescent staining of mouse cerebellum with Bergmann glia marker S100. TG mice treated with L-BMX or SAHA could reduce the Bergmann glia loss in their cerebella. Scale bar = 40 μm.

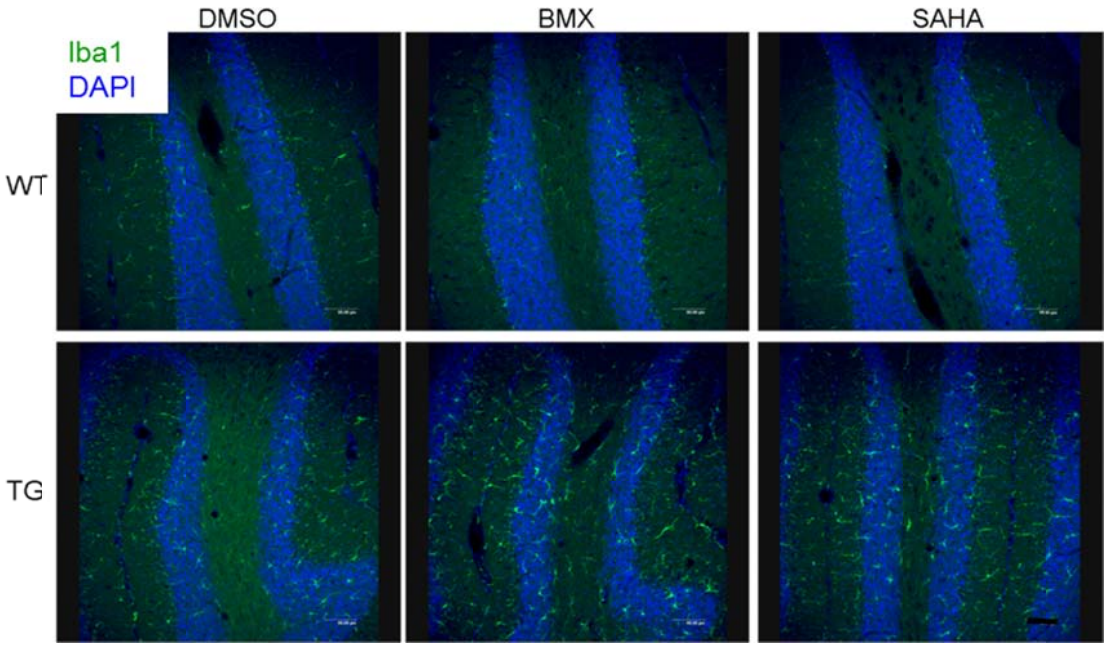
DMSO
BMX
SAHA
Iba1
DAPI
WT
TG

Figure 16. Inflammation level of cerebellum after mice treated with HDACi compounds.

Cerebellar sagittal-sections were stained for nuclei with DAPI (blue) and for microglia (Iba1, green).Immunofluorescent staining of mouse cerebellum with microglia marker Iba1. TG mice treated with L-BMX or SAHA showed stimulation in microglia activation in their cerebella. Scale bar = 40 μm.